ChemPhotoChem

Supporting Information

Substituent Effect on the Circularly Polarized Luminescence of C_1-Symmetric Carbene-Copper(I) Complexes

Erin E. Braker[+], Nishya F. M. Mukthar[+], Nathan D. Schley, and Gaël Ung*

Substituent Effect on the Circularly Polarized Luminescence of C1-Symmetrical Carbene-Copper(I) Complexes

Table of Contents

General Information

Synthesis

All syntheses were performed in a glovebox under N_2 atmosphere unless stated otherwise. All solvents, excluding toluene, were dried using a solvent purification system from Pure Process Technologies. Toluene was dried via reflux over elemental sodium.

Photophysical Characterization

Absorption spectra were collected with a Horiba Duetta spectrophotometer using the EZSpec software. CPL spectra were collected on an OLIS CPL Solo using the GlobalWorks software. Quantum yields were determined using a reference method, utilizing 1,9-diphenylanthracene as an external standard. Lifetime data were collected using the OLIS CPL Solo along with GlobalWorks and Photon Counting Phosphorescence (PCPH). All measurements were taken in sealed, quartz cuvettes under N_2 atmosphere. NMR spectra were collected with a Bruker AVANCE III 400MHz spectrometer under N_2.

X-ray Crystallography

Single-crystal X-ray diffraction studies were performed at Vanderbilt University: a suitable crystal of each sample was selected for analysis and mounted in a polyimide loop. All measurements were made on a Rigaku Oxford Diffraction Supernova Eos CCD with filtered Cu Kα or Mo Kα radiation at a temperature of 100 K. Using Olex2,[1] the structure was solved with the ShelXT structure solution program using direct methods and refined with the ShelXL refinement package[2] using least squares minimization.

Synthesis and Characterization

^{DMent}CAAC-Cu-F: The product was synthesized using a previously described method by Hall et al. and matched the previously reported spectroscopic data.[3]

^{DMent}CAAC-Cu-Br: A suspension of copper(I) bromide (143.45 g mol^{-1}, 0.075 g, 0.52 mmol, 1.1 eq) in 6 mL of tetrahydrofuran (THF) was prepared in a 20 mL scintillation vial equipped with a stir bar. A solution of ^{DMent}CAAC (382.66 g mol^{-1}, 0.181 g, 0.47 mmol, 1 eq) in 2 mL THF was added to the suspension and the reaction mixture was left to stir overnight. The resulting suspension was then filtered over Celite and the resulting filtrate was concentrated under vacuum to an off-white powder which was further washed with pentane to yield the product as a white powder (525.11 g mol^{-1}, 0.215 g, 0.41 mmol, 87%). ^{1}H NMR (C_6D_6, 400 MHz): *δ (ppm)* 7.10 (t, *J* = 7.7 Hz, 1H), 6.99 (t, *J* = 8.0 Hz, 2H), 3.09 – 2.85 (m, 2H), 2.78 (sept, *J* = 6.7 Hz, 2H), 2.07 (m, 1H), 1.85 (d, *J* = 14 Hz, 1H), 1.79 – 1.64 (m, 3H), 1.47 (d, *J* = 6.8 Hz, 3H), 1.43 (d, *J* = 6.6 Hz, 3H), 1.31 – 1.17 (m, 5H), 1.16 – 0.97 (m, 11H), 0.95 – 0.86 (m, 11H), 0.83 (d, *J* = 6.4 Hz, 3H). ^{13}C NMR (C_6D_6, 101 MHz): *δ (ppm)* 251.8, 145.6, 145.2, 135.4, 129.9, 125.0, 124.8, 77.1, 65.2, 52.8, 51.4, 48.1, 35.8, 31.0, 29.4, 29.3, 29.0, 28.8, 27.9, 27.7, 26.8, 25.1, 24.3, 23.0, 22.5, 22.4, 20.0. Anal. Calcd for $C_{27}H_{43}BrCuN$: C, 61.76; H, 8.25; N, 2.67. Found: C, 61.70; H, 8.20; N, 2.64.

The product was recrystallized via slow diffusion of THF into toluene.

^{DMent}CAAC-Cu-I: The product was prepared and recrystallized analogously to ^{DMent}CAAC-Cu-Br substituting copper(I) iodide (MW 190.45 g mol^{-1}, 0.030 g, 0.16 mmol, 1.1 eq) for copper(I) bromide to yield the product as a white powder (572.11 g mol^{-1}, 0.087 g, 0.15 mmol, 97%). ^{1}H NMR (C_6D_6, 400 MHz): *δ (ppm)* 7.11 (t, *J* = 7.7 Hz, 1H), 7.01 (td, *J* = 7.3, 1.7 Hz, 2H), 2.96 (m, 2H), 2.78 (sept, *J* = 7.0 Hz, 2H), 2.08 (m, 1H), 1.89 (d, *J* = 14 Hz, 1H), 1.77 (m, 3H), 1.48 (d, *J* = 6.8 Hz, 3H), 1.44 (d, *J* = 6.7 Hz, 3H), 1.28 (m, 2H), 1.17 – 1.04 (m, 10H), 0.98 – 0.86 (m, 10H), 0.82 (d, *J* = 6.4 Hz, 3H). ^{13}C NMR (C_6D_6, 101 MHz): *δ (ppm)* 252.6, 145.6, 145.1, 135.4, 129.9, 125.0, 124.9, 77.5, 65.5, 52.7, 51.4, 47.9, 35.8, 30.9, 29.4, 29.3, 29.0, 28.8, 27.9, 27.9, 27.0, 25.2, 24.2, 23.0, 22.7, 22.6, 20.0. Anal. Calcd for $C_{27}H_{43}ICuN$: C, 56.69; H, 7.58; N, 2.45. Found: C, 56.60; H, 7.52; N, 2.44.

^{DMent}CAAC-Cu-BH_4**:** The product was prepared and recrystallized analogously to ^{DMent}CAAC-Cu-B_3H_8 substituting KB_3H_8 with $NaBH_4$ (37.83 g mol^{-1}, 0.024 g, 0.6 mmol, 4.2 eq) to yield the product as a fluffy, white powder (459.59 g mol^{-1}, 0.062 g, 0.13 mmol, 84%). ^{1}H NMR (C_6D_6, 400 MHz): *δ (ppm)* 7.11 (t, *J* = 7.8 Hz, 1H), 6.99 (m, 2H), 3.07 – 2.85 (m, 2H), 2.78 (sept, *J* = 6.8 Hz, 2H), 2.03 (m, 1H), 1.86 (d, *J* = 14 Hz, 1H), 1.80 – 1.63 (m, 3H), 1.43 (d, *J* = 6.8 Hz, 3H), 1.39 (d, *J* = 6.7 Hz, 3H), 1.33 – 1.27 (m, 3H), 1.17 – 1.04 (m, 10H), 0.98 – 0.86 (m, 10H), 0.83 (d, *J* = 6.5 Hz, 3H), 0.50 (q [br], 4H). ^{13}C NMR (C_6D_6, 101 MHz): *δ (ppm)* 251.8, 145.6, 145.2, 135.5, 129.9, 125.0, 124.8, 77.2, 65.3, 52.7, 51.3, 48.1, 35.8, 31.0, 29.3, 29.0, 28.8, 27.9, 27.7, 26.8, 25.1, 24.3, 23.0, 22.6, 22.5, 20.0. ^{11}B NMR (C_6D_6, 128.38 MHz): *δ (ppm)* -39.12 (quint.). Anal. Calcd for $C_{27}H_{47}BCuN$: C, 70.49; H, 10.30; N, 3.04. Found: C, 70.44; H, 10.25; N, 2.99.

The product was recrystallized by slow diffusion of pentane into 2-MeTHF.

^{DMent}CAAC-Cu-B_3H_8**:** ^{DMent}CAAC-Cu-Br (525.11 g mol^{-1}, 0.079 g, 0.15 mmol, 1 eq) was transferred to a vial and suspended in THF (6 mL).[4] A solution of KB_3H_8 (79.59 g mol^{-1}, 0.026 g, 0.327 mmol, 2.2 eq) in THF (2 mL) was added slowly to the suspension while stirring. The reaction mixture was left to stir overnight. The resulting solution was filtered over Celite and concentrated under vacuum to yield a white powder (486.70 g mol^{-1}, 0.066 g, 0.14 mmol, 90%). ^{1}H NMR (C_6D_6, 400 MHz): *δ (ppm)* 7.08 (t, *J* = 7.8 Hz, 1H), 6.98 (m, 2H), 2.81 (m, 2H), 2.66 (m, 1H), 2.32 (m, 1H), 1.99 (m, 1H), 1.89 (d, *J* = 14 Hz, 1H), 1.86 – 1.60 (m, 3H), 1.44 – 1.28 (m, 6H), 1.24 (d, *J* = 13 Hz, 2H), 1.17 – 1.04 (m, 10H), 0.98 – 0.86 (m, 10H), 0.85 – 0.36 (br, 8H). ^{13}C NMR (C_6D_6, 101 MHz): *δ (ppm)* 247.0, 145.9, 145.3, 136.0, 129.7, 125.3, 125.3, 77.5, 65.8, 52.7, 52.0, 48.5, 35.5, 31.0, 29.7, 29.5, 29.1, 28.9, 27.9, 27.3, 26.8, 25.2, 24.5, 23.7, 23.7, 22.9, 19.8. ^{11}B NMR (C_6D_6, 128.38 MHz): *δ (ppm)* -35.84 (s). Anal. Calcd for $C_{27}H_{51}B_3CuN$: C, 66.77; H, 10.58; N, 2.88. Found: C, 66.70; H, 10.50; N, 2.84.

The product was recrystallized via slow diffusion of THF into pentane.

[^{DMent}CAAC-Cu-H]$_2$: The product was synthesized using a previously described method by Frey et al. and matched the previously reported spectroscopic data.[5]

^{LMent}CAAC-Cu-F**:** The product was synthesized using a previously described method by Hall et al. and matched the previously reported spectroscopic data.[3]

^{LMent}CAAC-Cu-Br**:** The product was prepared analogously to its enantiomer using the L enantiomer (382.66 g mol^{-1}, 0.060 g, 0.16 mmol, 1 eq) to yield the product as a fluffy, white powder (525.11 g mol^{-1}, 0.069 g, 0.13 mmol, 84%). Spectroscopic data matched those of its enantiomer.

^{LMent}CAAC-Cu-I**:** The product was prepared analogously to its enantiomer using the L enantiomer (382.66 g mol^{-1}, 0.060 g, 0.16 mmol, 1 eq) to yield the product as a fluffy, white powder (572.11 g mol^{-1}, 0.086 g, 15 mmol, 98%). Spectroscopic data matched those of its enantiomer.

^{LMent}CAAC-Cu-BH_4**:** The product was prepared analogously to its enantiomer using the L enantiomer (525.11 g mol^{-1}, 0.054 g, 0.10 mmol, 1 eq) to yield the product as a fluffy, white powder (459.59 g mol^{-1}, 0.035 g, 0.08 mmol, 74%). Spectroscopic data matched those of its enantiomer.

^{LMent}CAAC-Cu-B_3H_8**:** The product was prepared analogously to its enantiomer using the L enantiomer (525.11 g mol^{-1}, 0.080 g, 0.15 mmol, 1 eq) to yield the product as a fluffy, white powder (486.70 g mol^{-1}, 0.065 g, 13 mmol, 87%). Spectroscopic data matched those of its enantiomer.

NMR Data

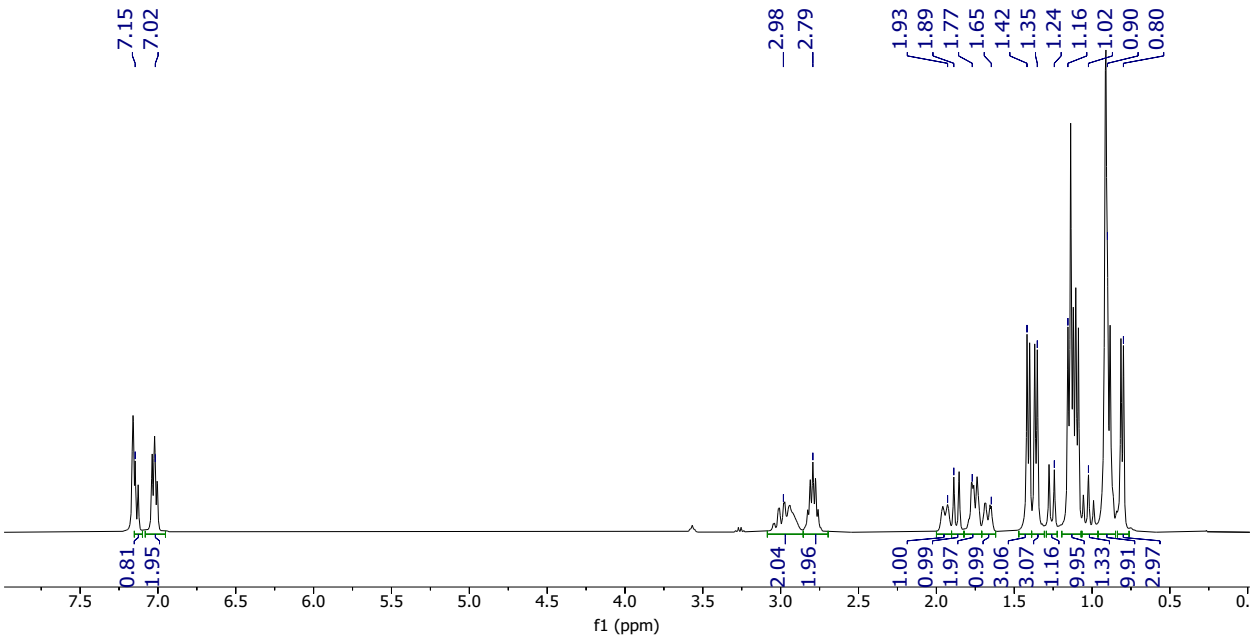

Figure S1. ^{1}H NMR of ^{D}-fluoride in C_6D_6

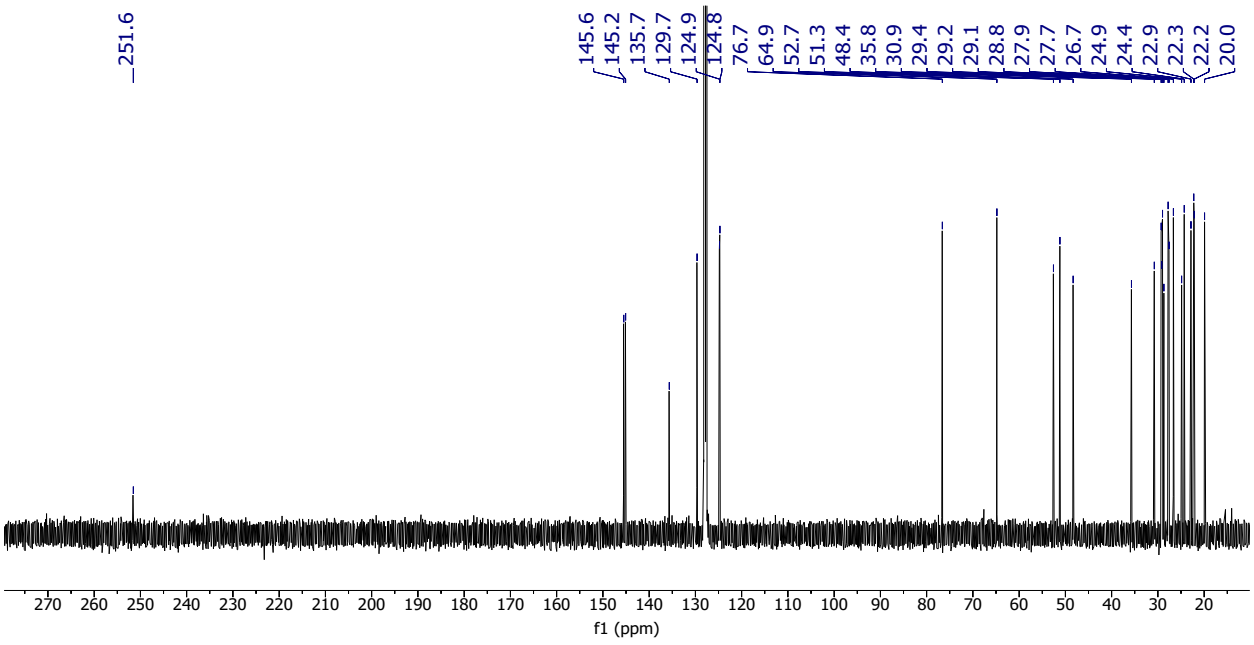

Figure S2. ^{13}C NMR of ^{D}-fluoride in C_6D_6

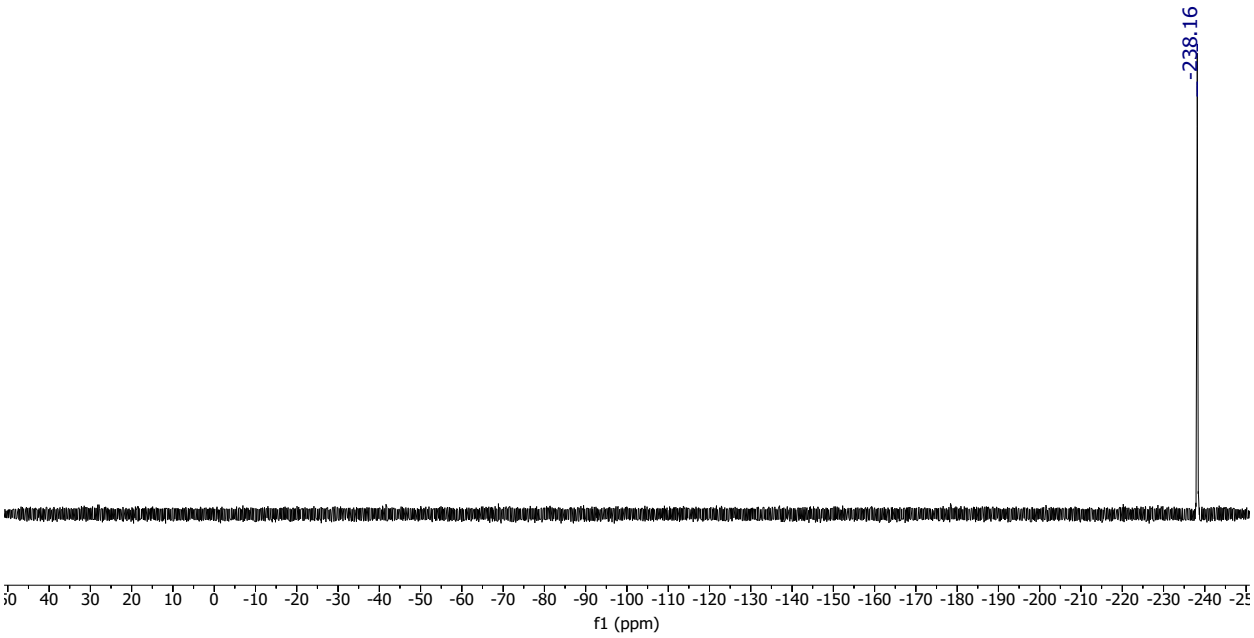

Figure S3. ^{19}F NMR of ^{D}-fluoride in C_6D_6

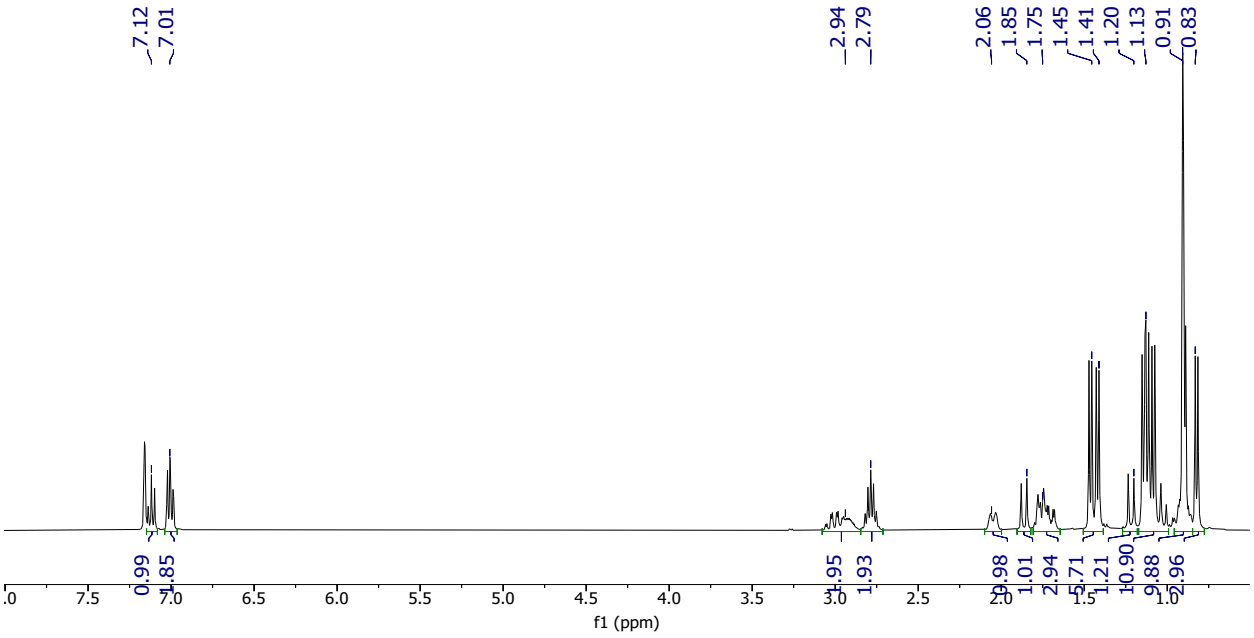

Figure S4. ^{1}H NMR of ^{D}-bromide in C_6D_6

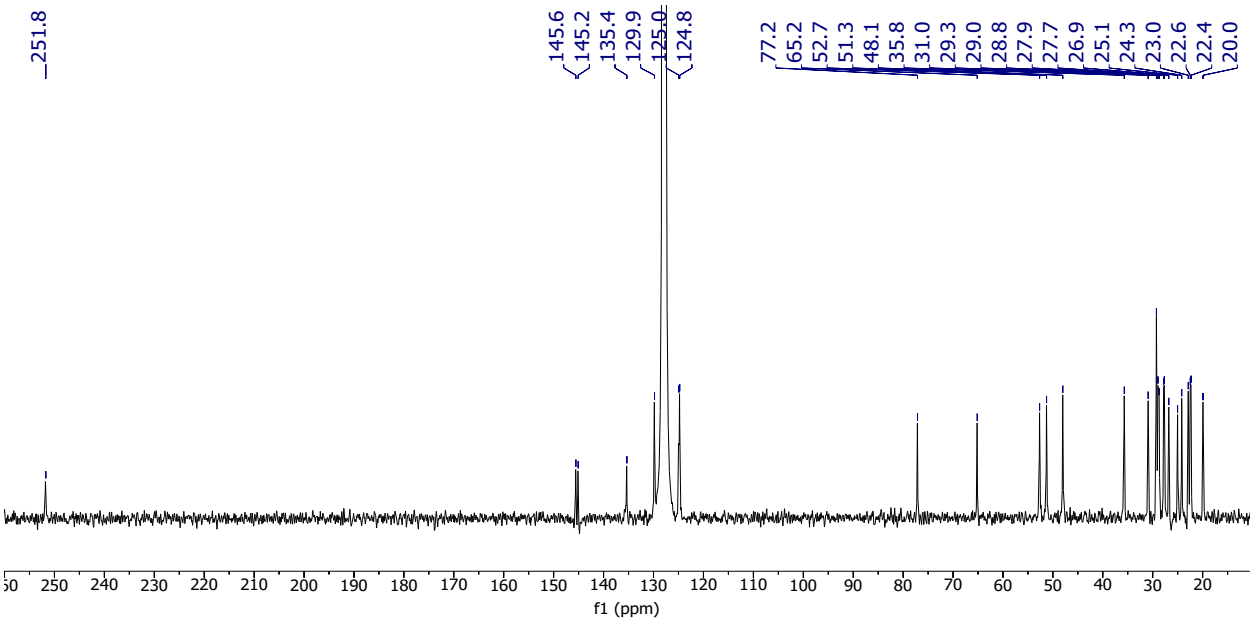

Figure S5. ^{13}C NMR of ^{D}-bromide in C_6D_6

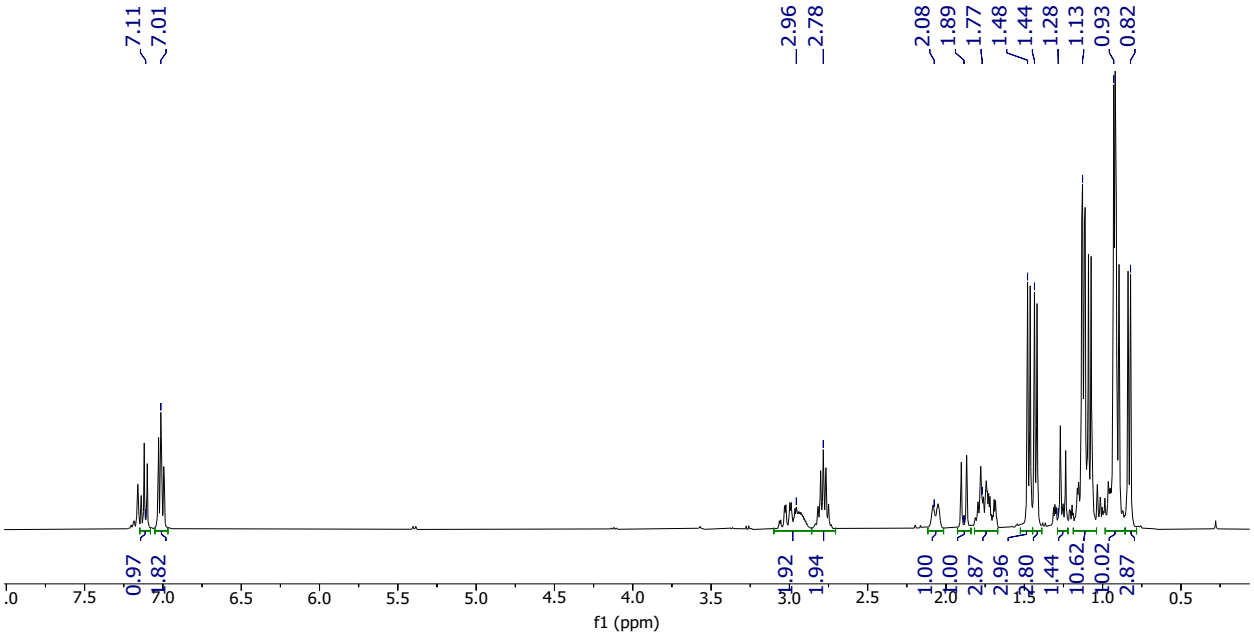

Figure S6. ^{1}H NMR of ^{D}-iodide in C_6D_6

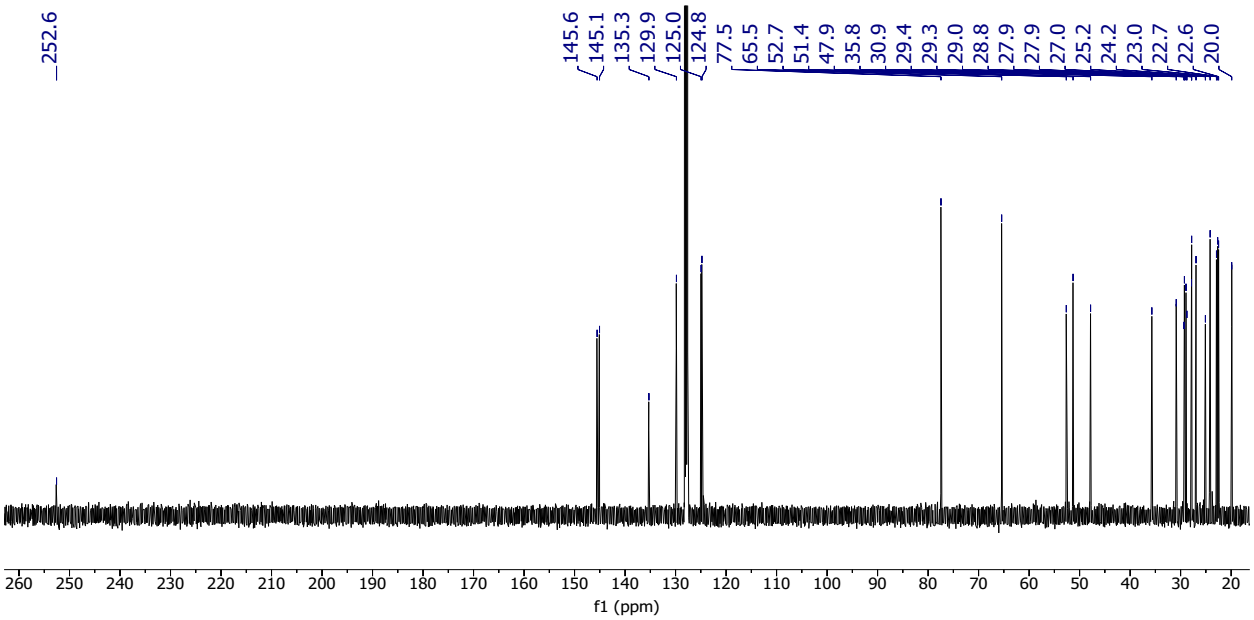

Figure S7. ^{13}C NMR of ^{D}-iodide in C_6D_6

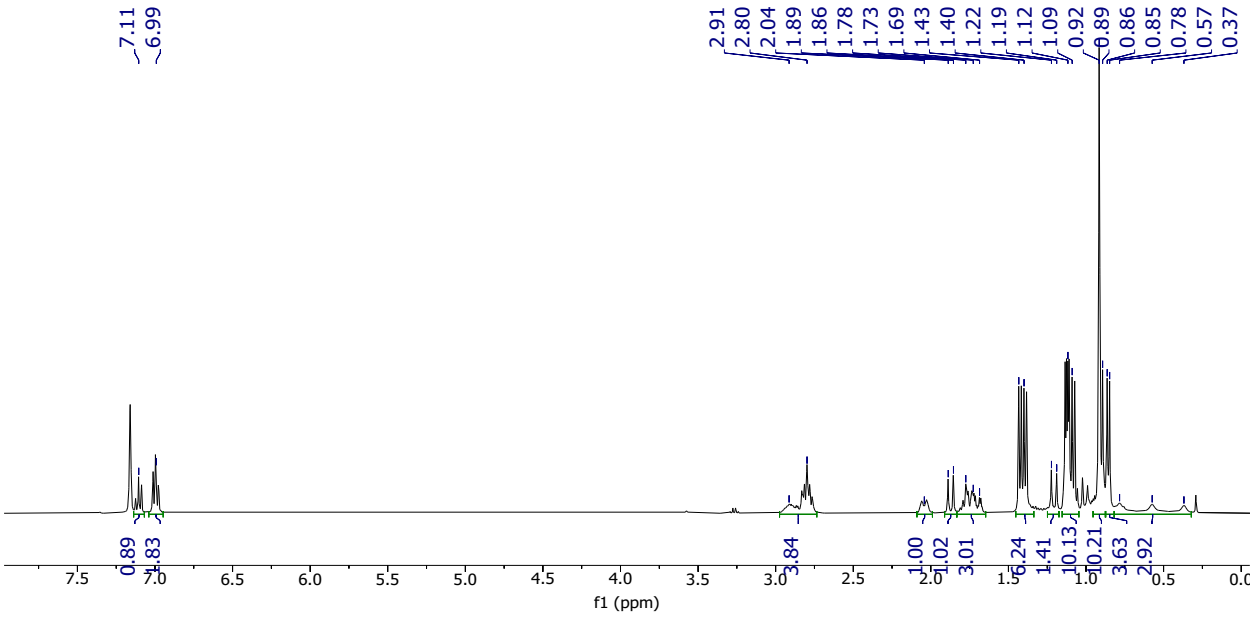

Figure S8. ^{1}H NMR of ^{D}-BH_4 in C_6D_6

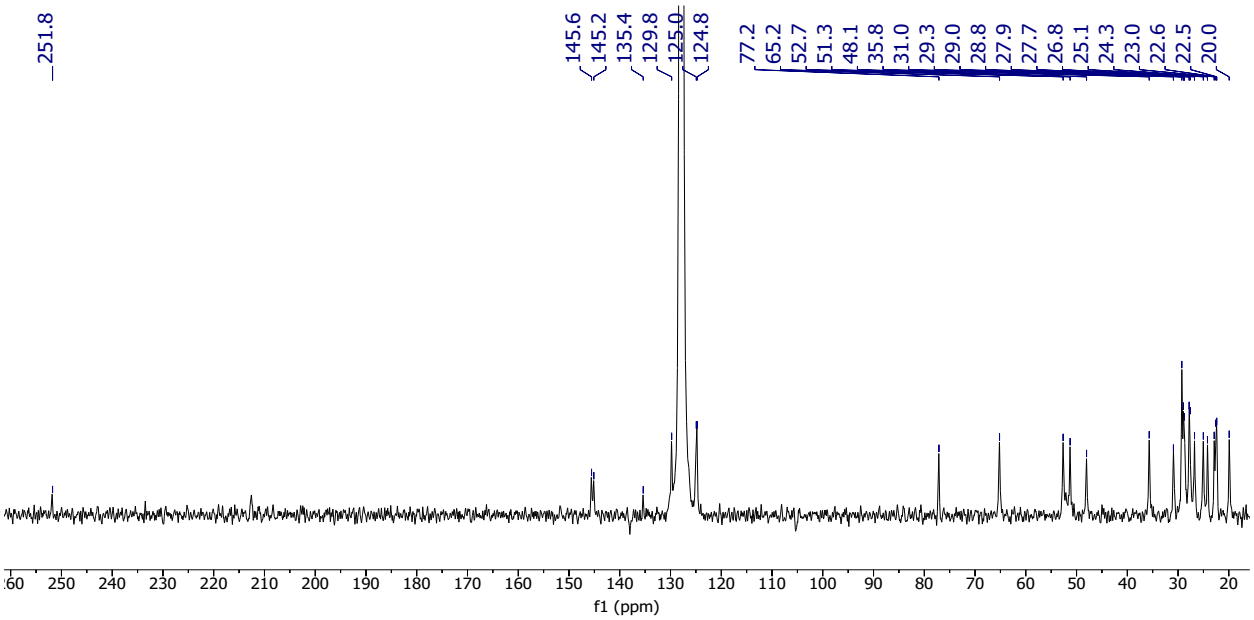

Figure S9. ^{13}C NMR of ^{D}-BH_4 in C_6D_6

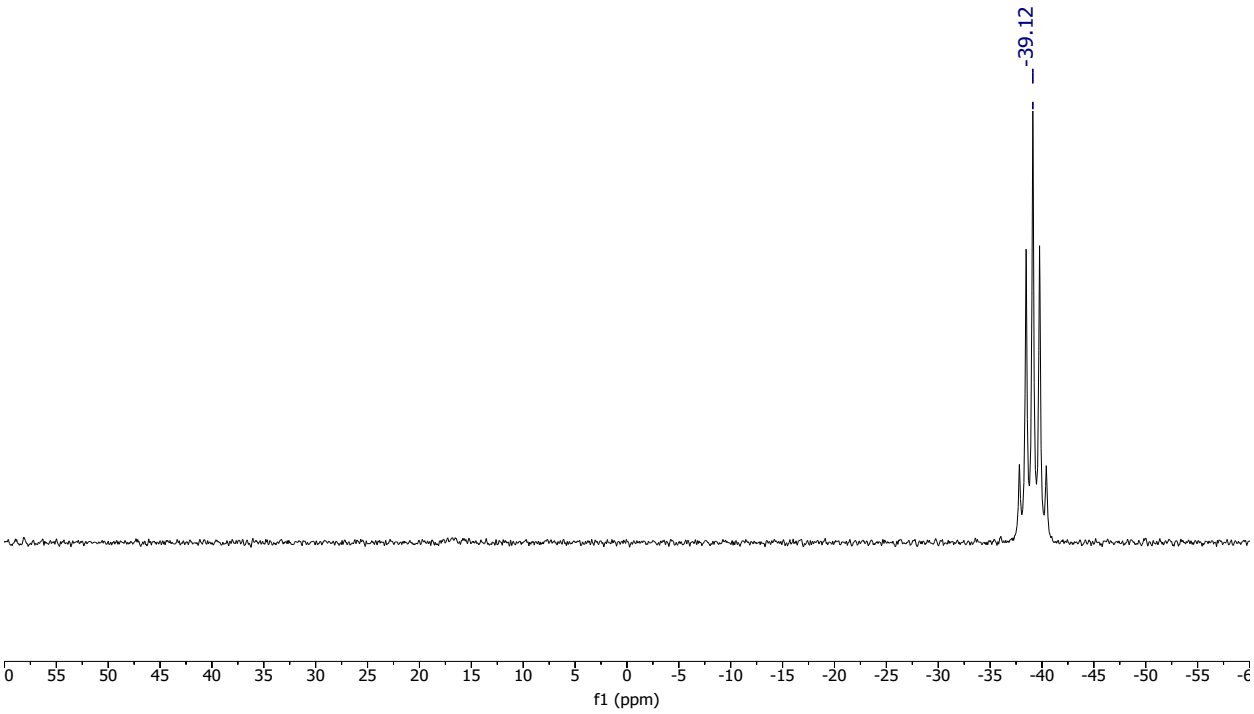

Figure S10. ^{11}B NMR of ^{D}-BH_4 in C_6D_6

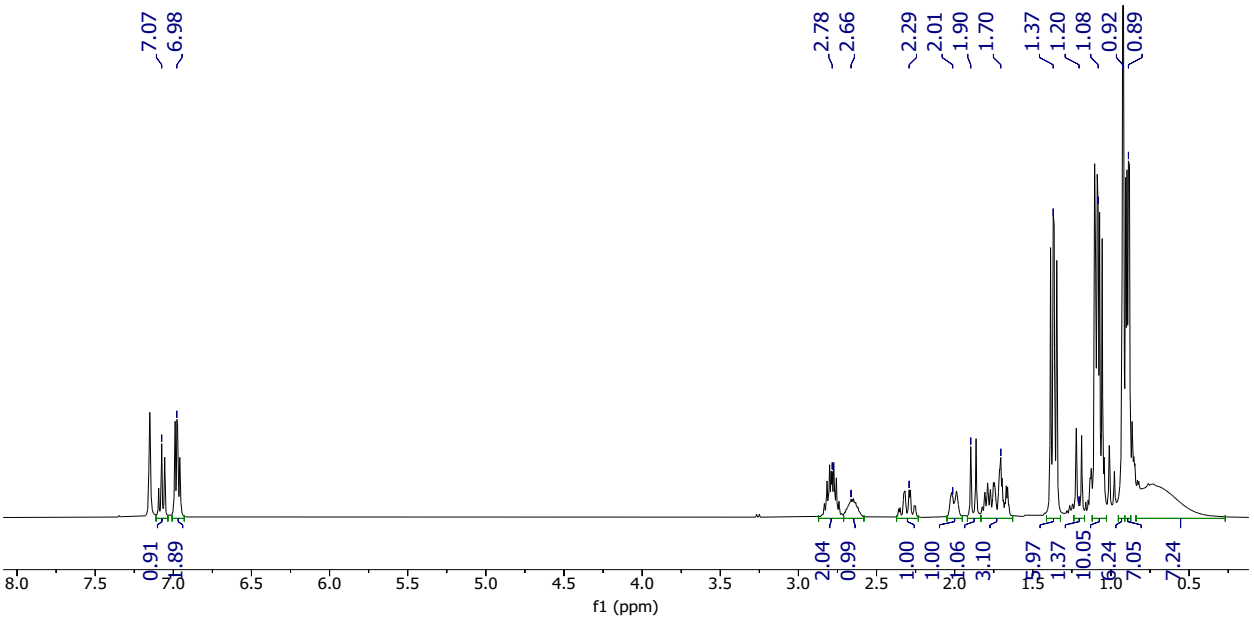

Figure S11. ^{1}H NMR of ^{D}-B_3H_8 in C_6D_6

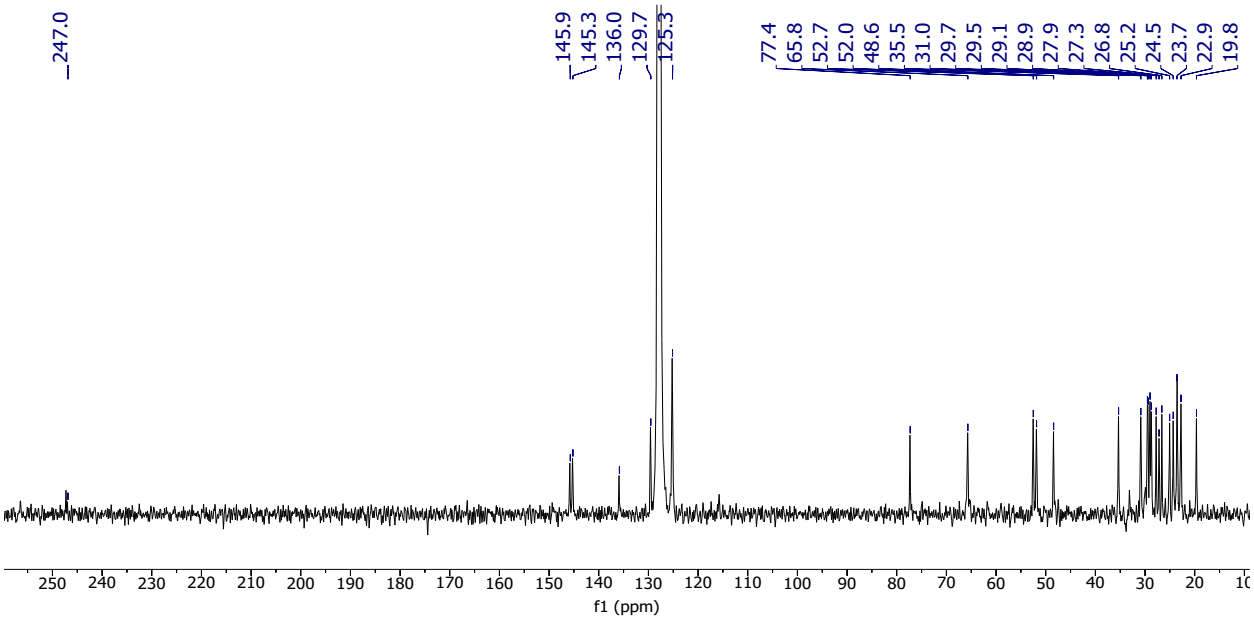

Figure S12. ^{13}C NMR of ^{D}-B_3H_8 in C_6D_6

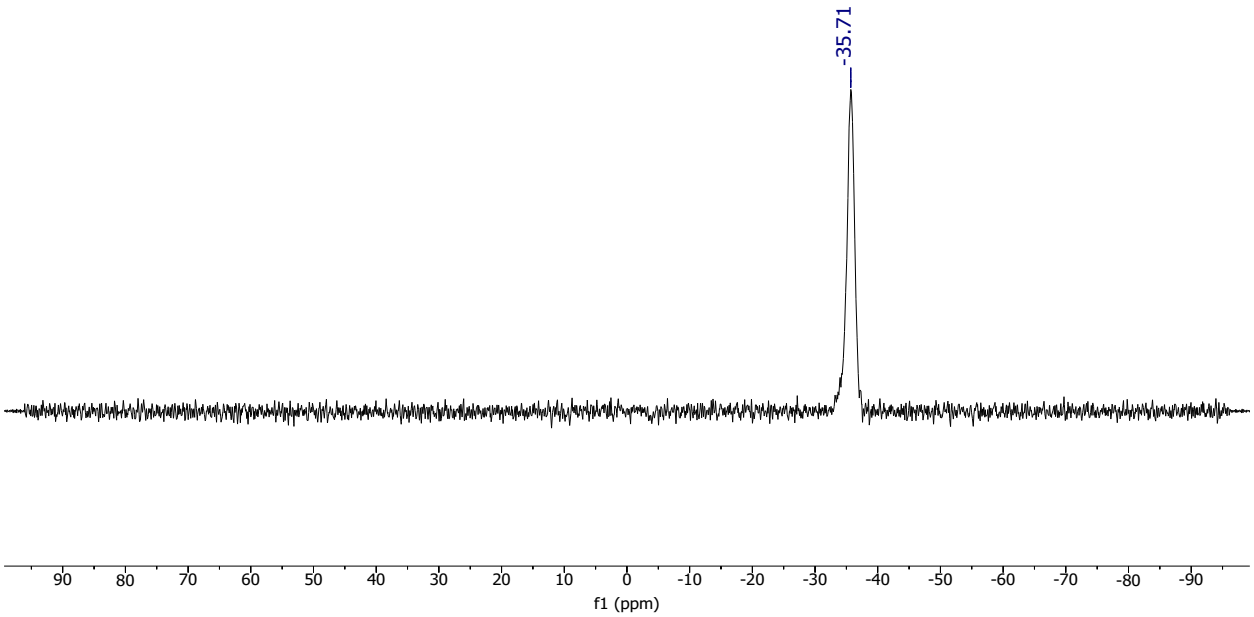

Figure S13. ^{11}B NMR of ^{D}-B_3H_8 in C_6D_6

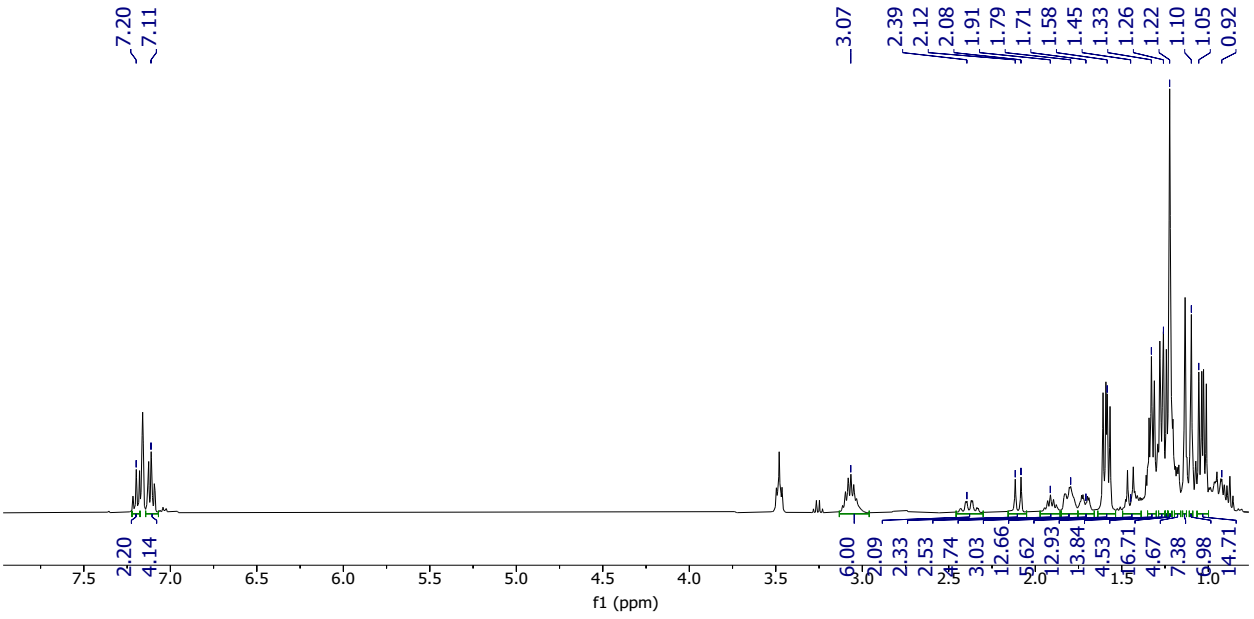

Figure S14. ^{1}H NMR of ^{D}-H in C_6D_6

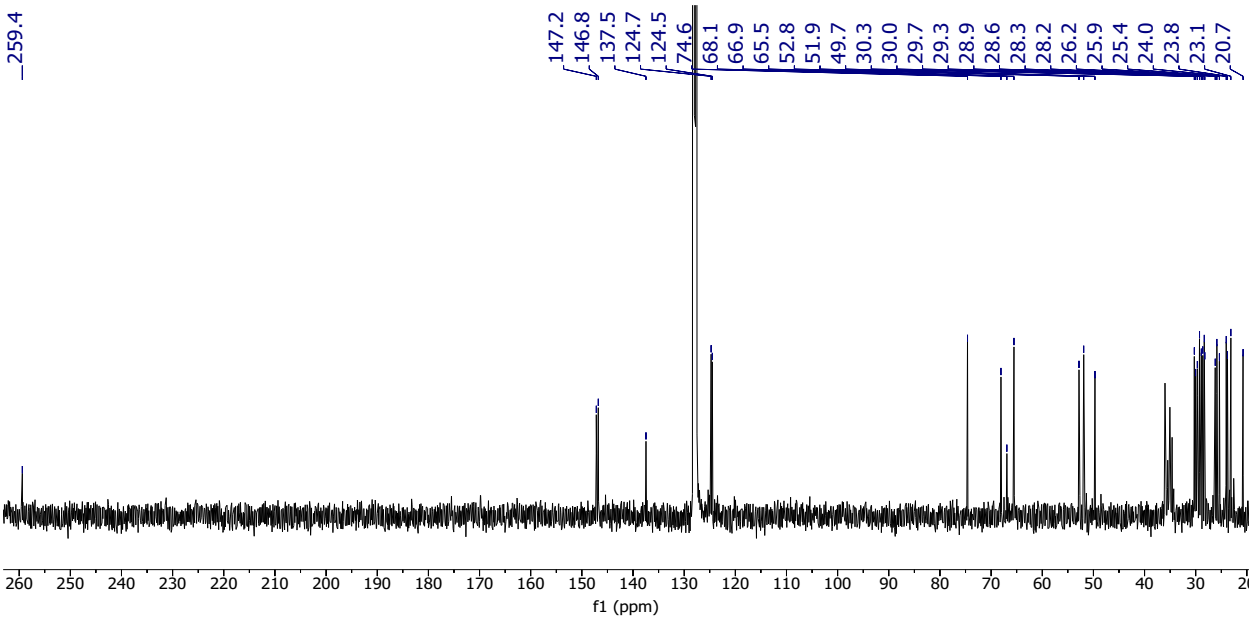

Figure S15. ^{13}C NMR of ^{D}-H in C_6D_6

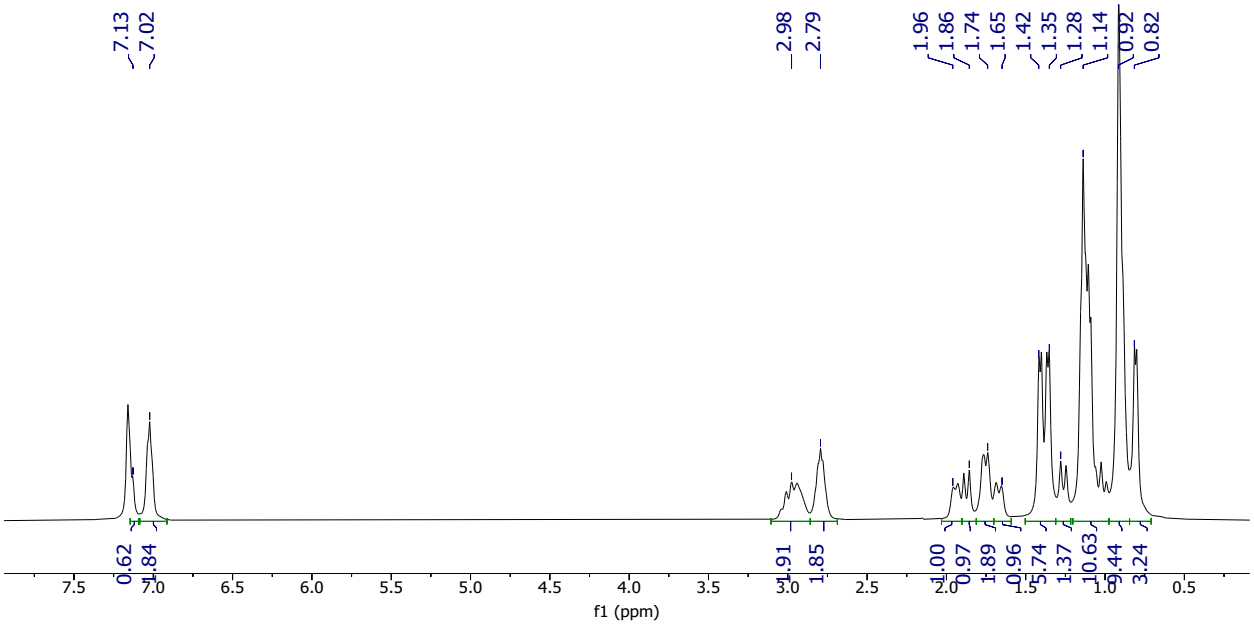

Figure S16. ^{1}H NMR of ^{L}-fluoride in C_6D_6

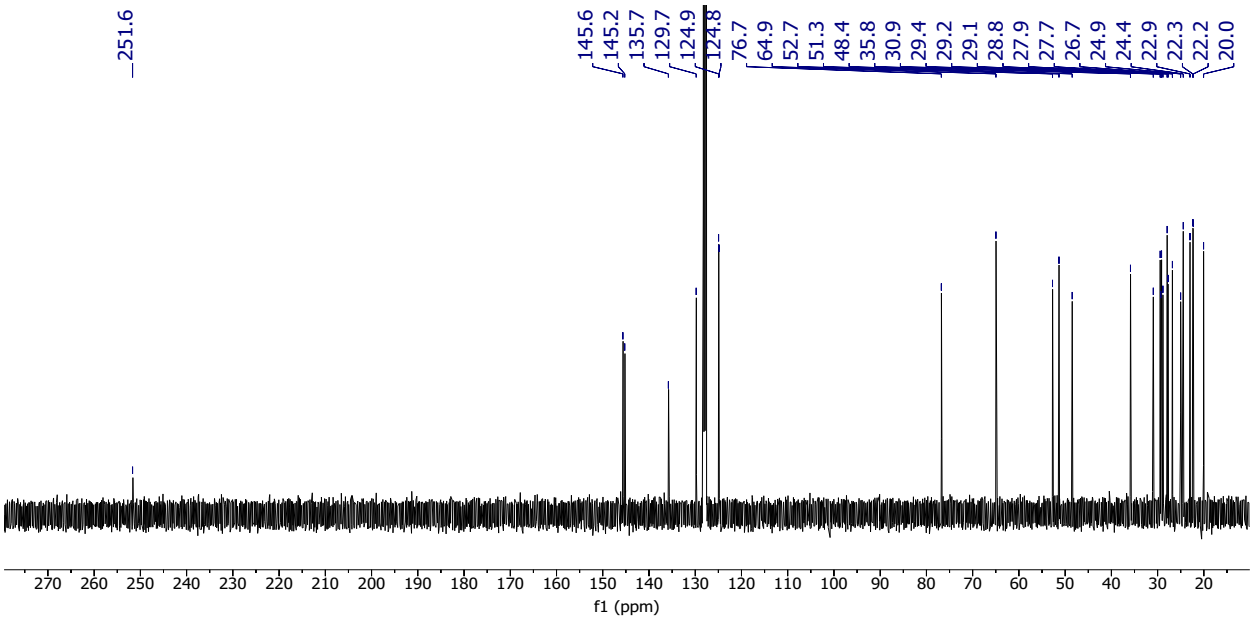

Figure S17. ^{13}C NMR of ^{L}-fluoride in C_6D_6

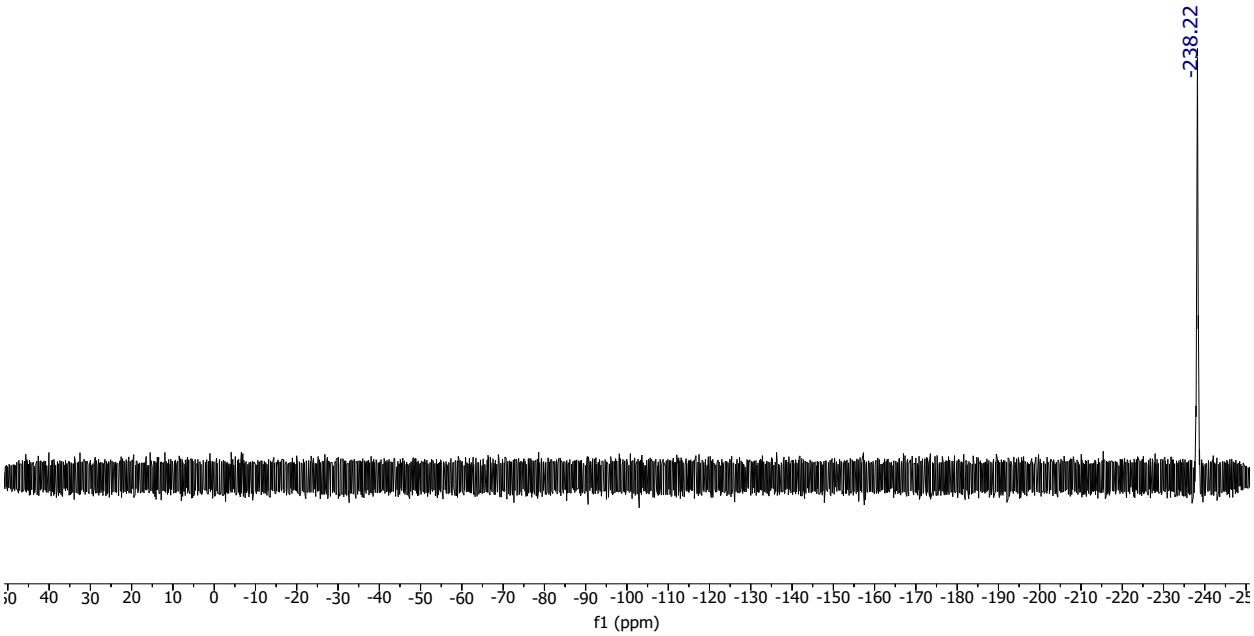

Figure S18. ^{19}F NMR of ^{L}-fluoride in C_6D_6

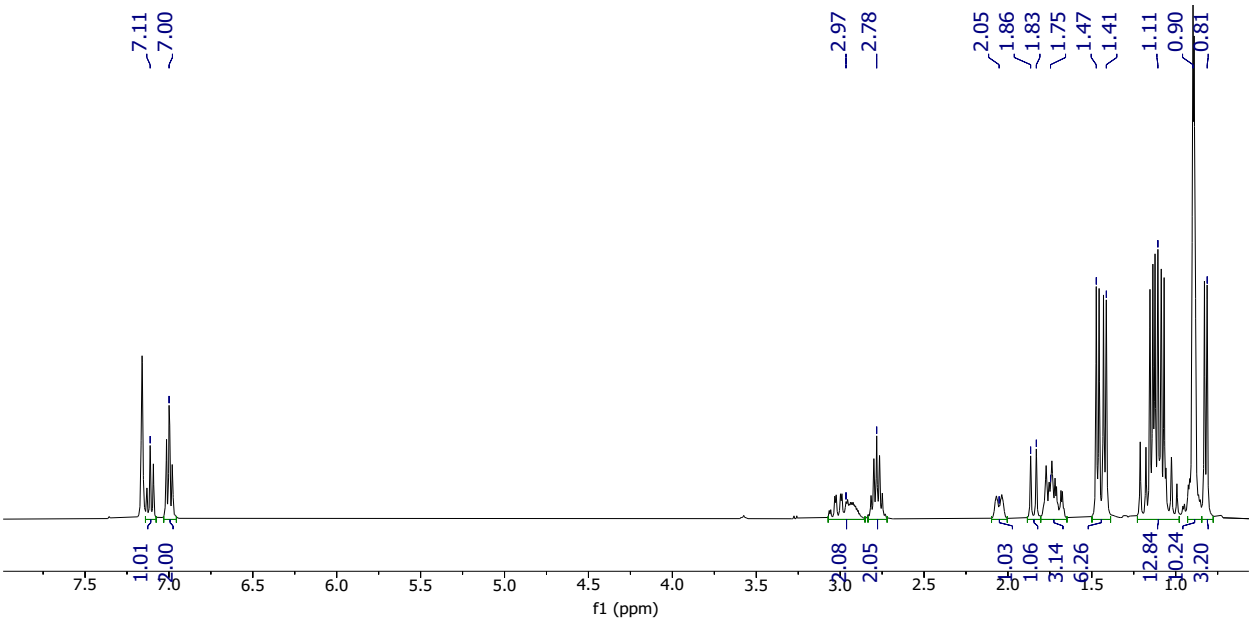

Figure S19. ^{1}H NMR of ^{L}-bromide in C_6D_6

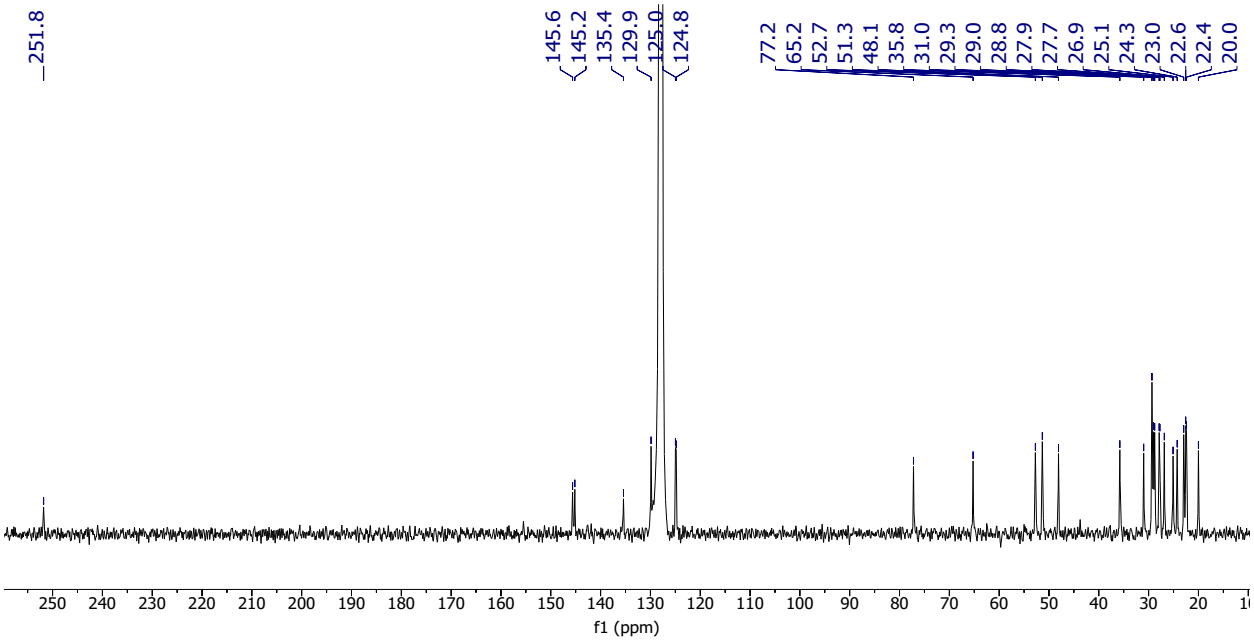

Figure S20. ^{13}C NMR of ^{L}-bromide in C_6D_6

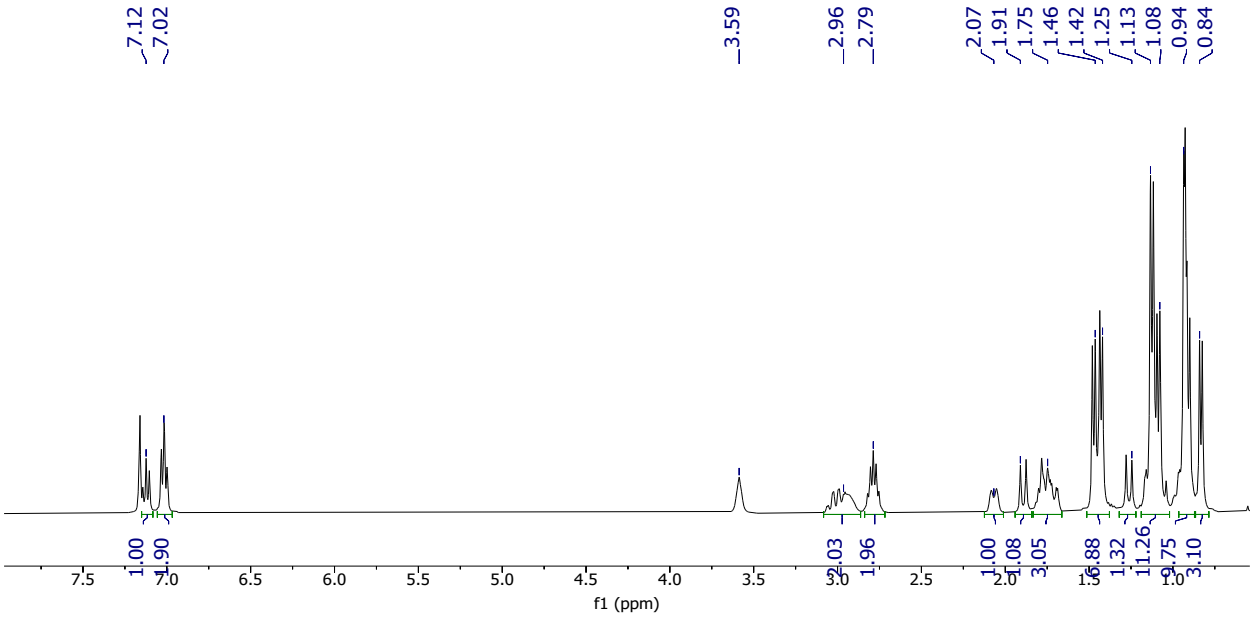

Figure S21. ^{1}H NMR of ^{L}-iodide in C_6D_6

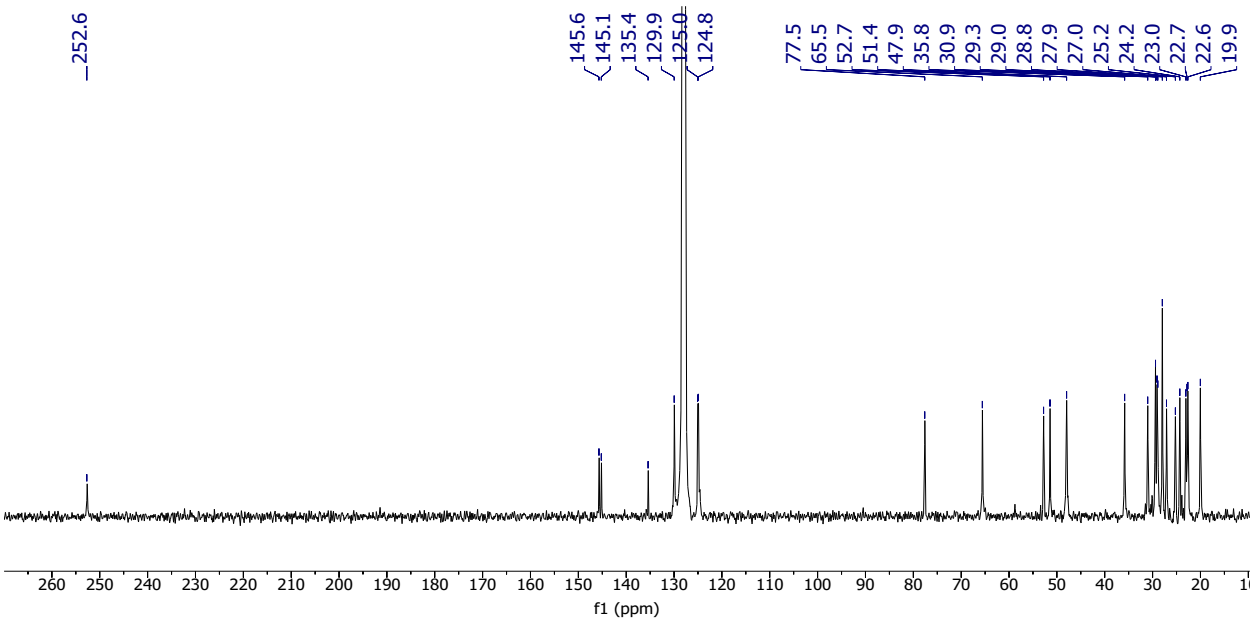

Figure S22. ^{13}C NMR of ^{L}-iodide in C_6D_6

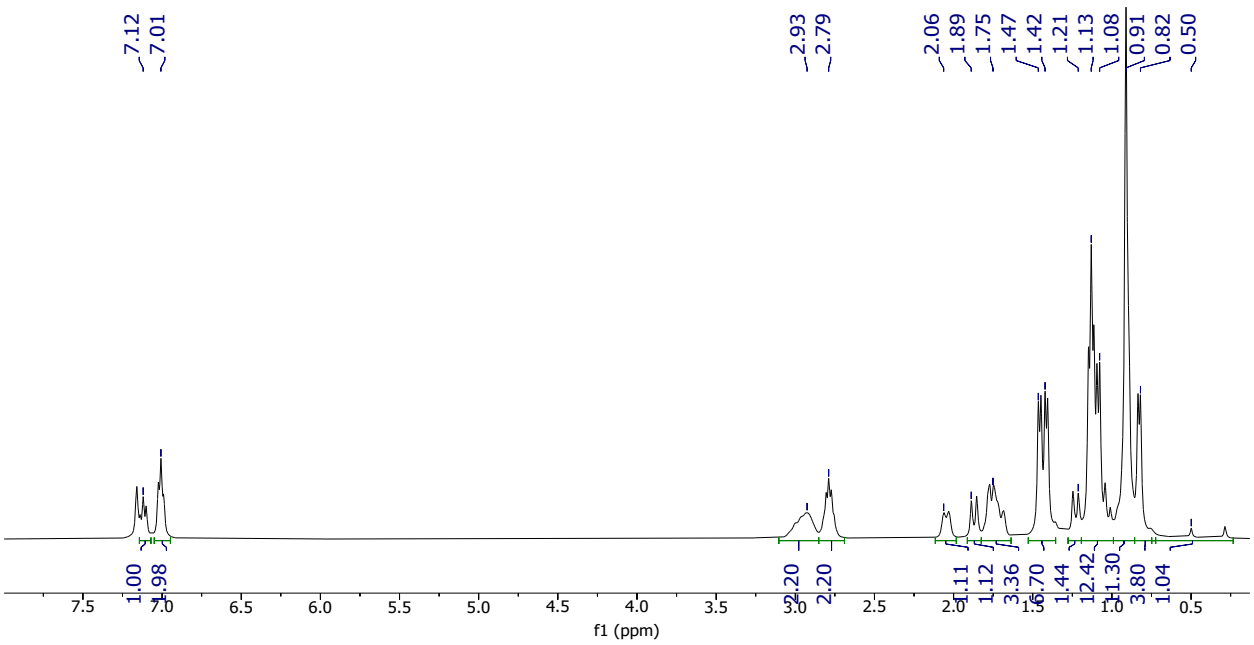

Figure S23. ^{1}H NMR of ^{L}-BH_4 in C_6D_6

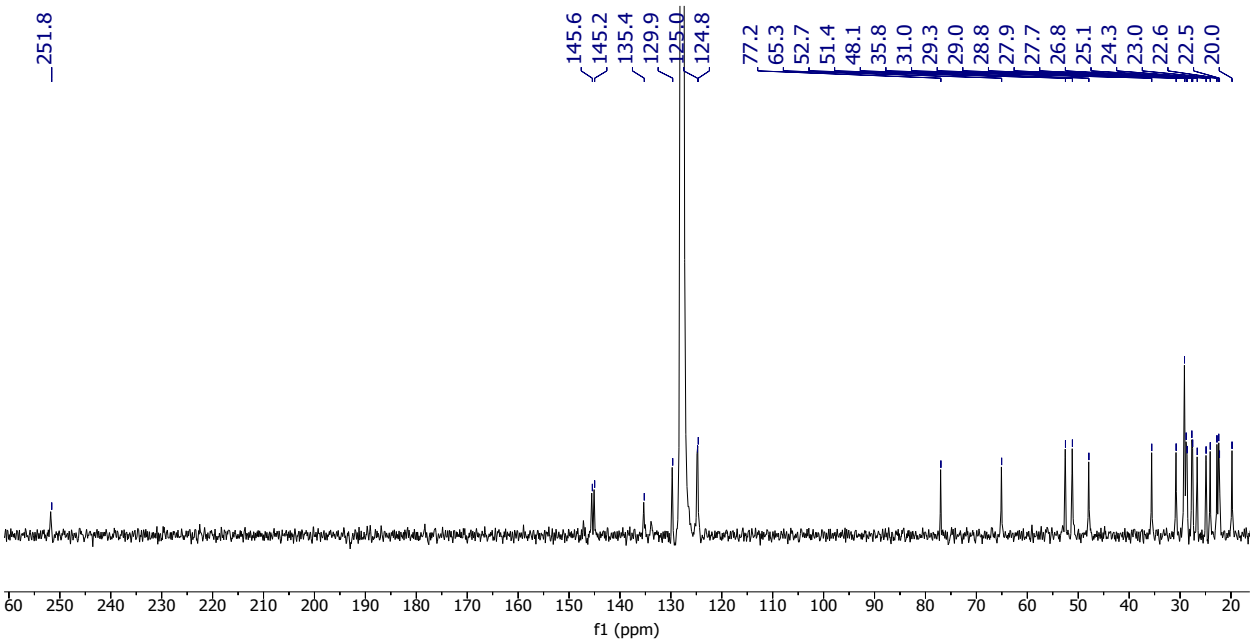

Figure S24. ^{13}C NMR of ^{L}-BH_4 in C_6D_6

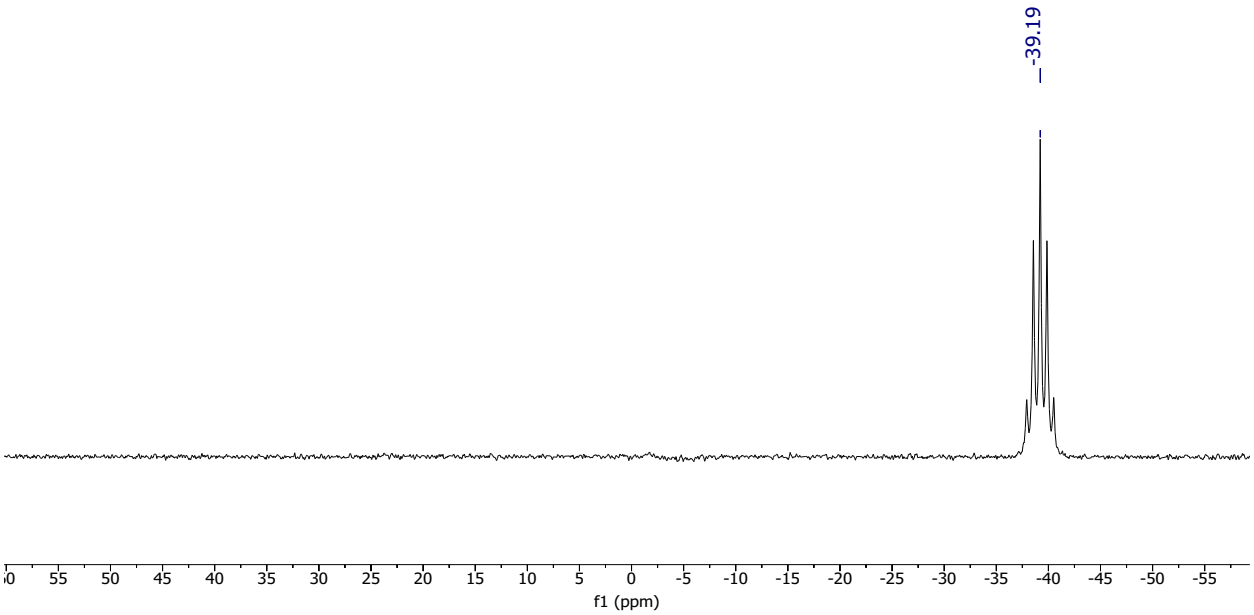

Figure S25. ^{11}B NMR of ^{L}-BH_4 in C_6D_6

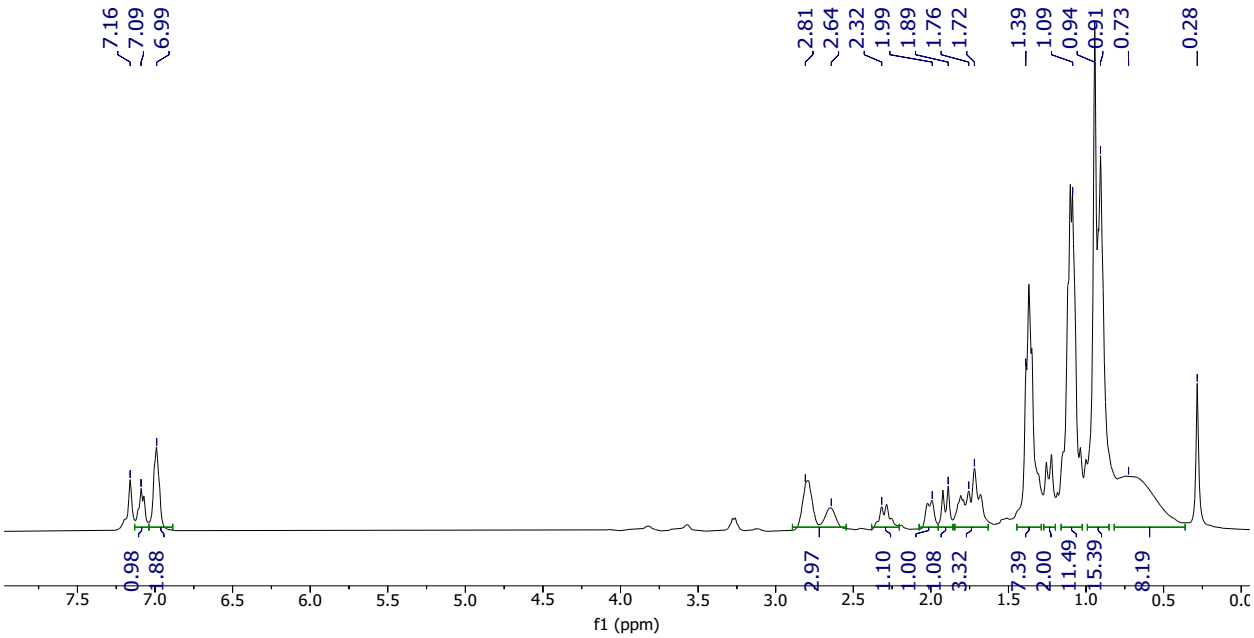

Figure S26. ^{1}H NMR of ^{L}-B_3H_8 in C_6D_6

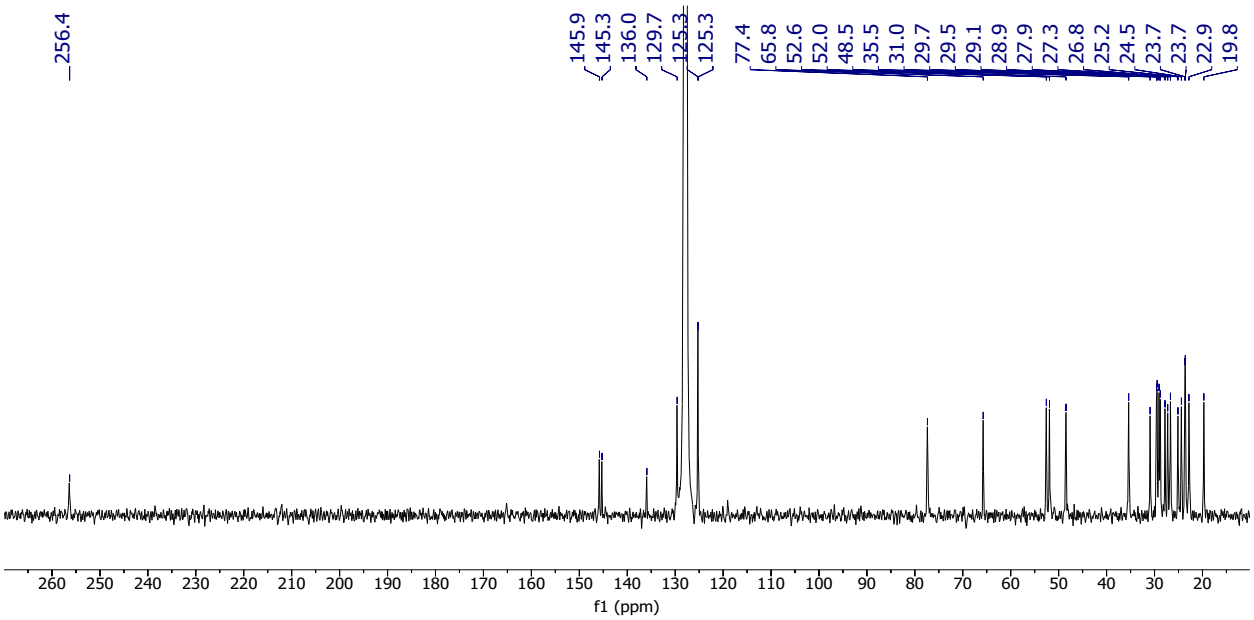

Figure S27. ^{13}C NMR of ^{L}-B_3H_8 in C_6D_6

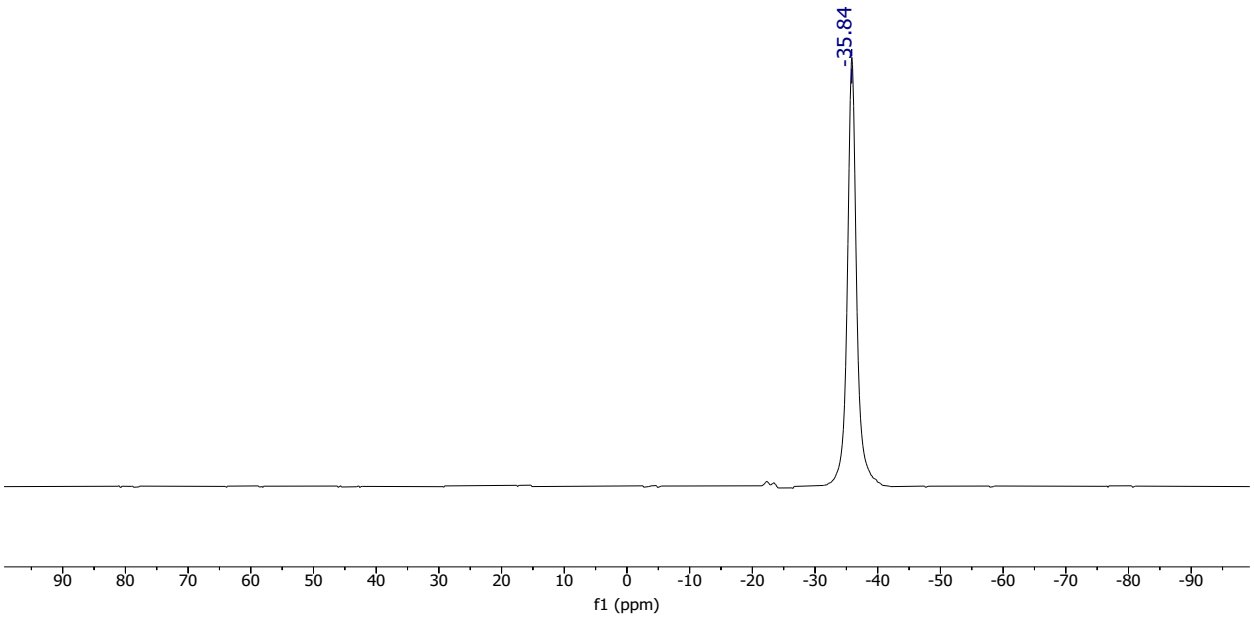

Figure S28. ^{11}B NMR of ^{L}-B_3H_8 in C_6D_6

Photophysical Data

CPL Measurements

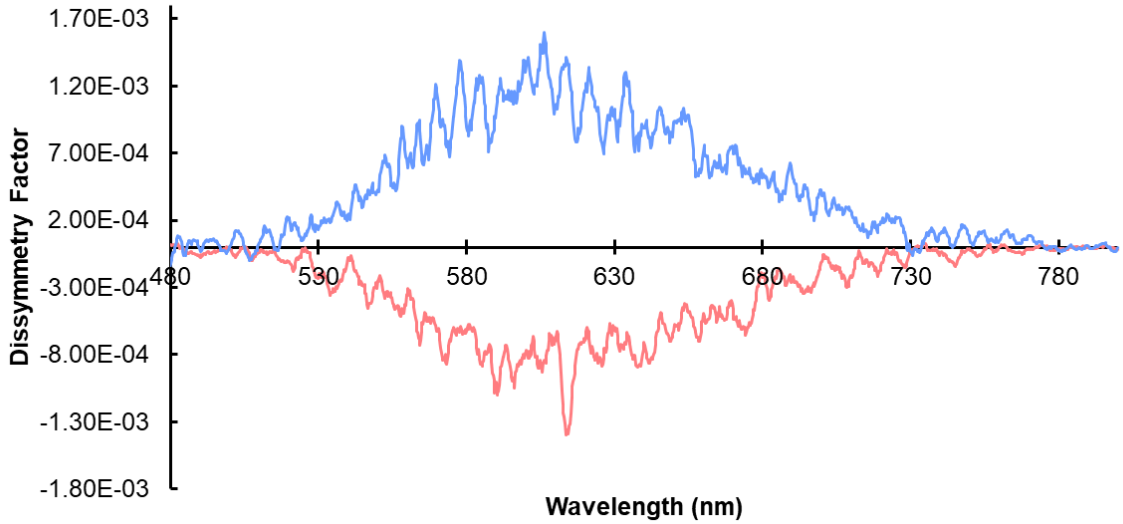

Figure S29. Normalized dissymmetry factor of ^{D}-fluoride (bottom, pink) and ^{L}-fluoride (top, blue) as a function of wavelength (5.0×10^{-3} mol L^{-1} in THF, λ_{ex} = 355 nm, band pass = 13 nm)

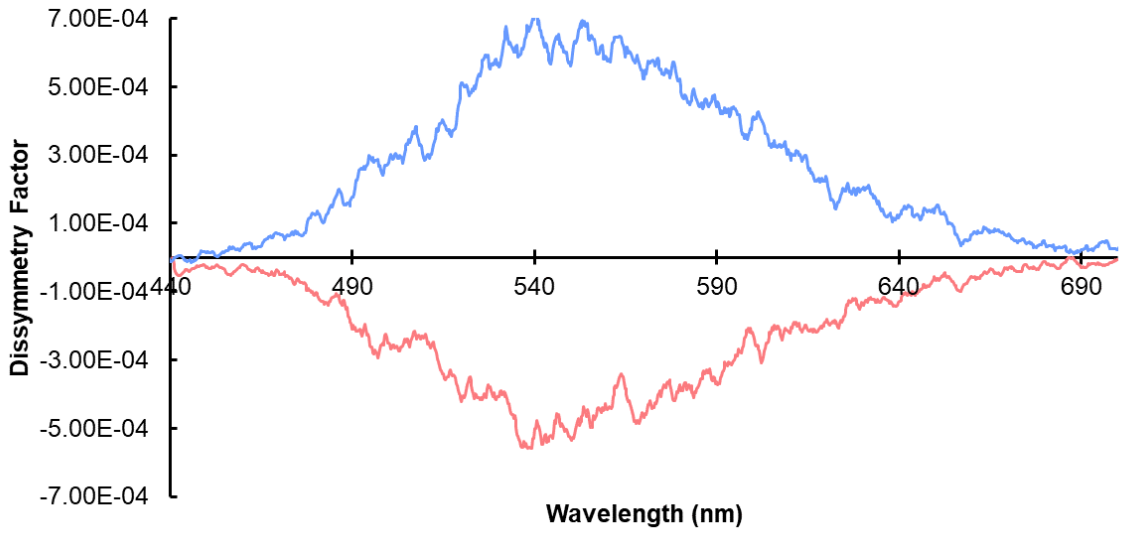

Figure S30. Normalized dissymmetry factor of ^{D}-bromide (bottom, pink) and ^{L}-bromide (top, blue) as a function of wavelength (5.0×10^{-3} mol L^{-1} in THF, λ_{ex} = 355 nm, band pass = 13 nm)

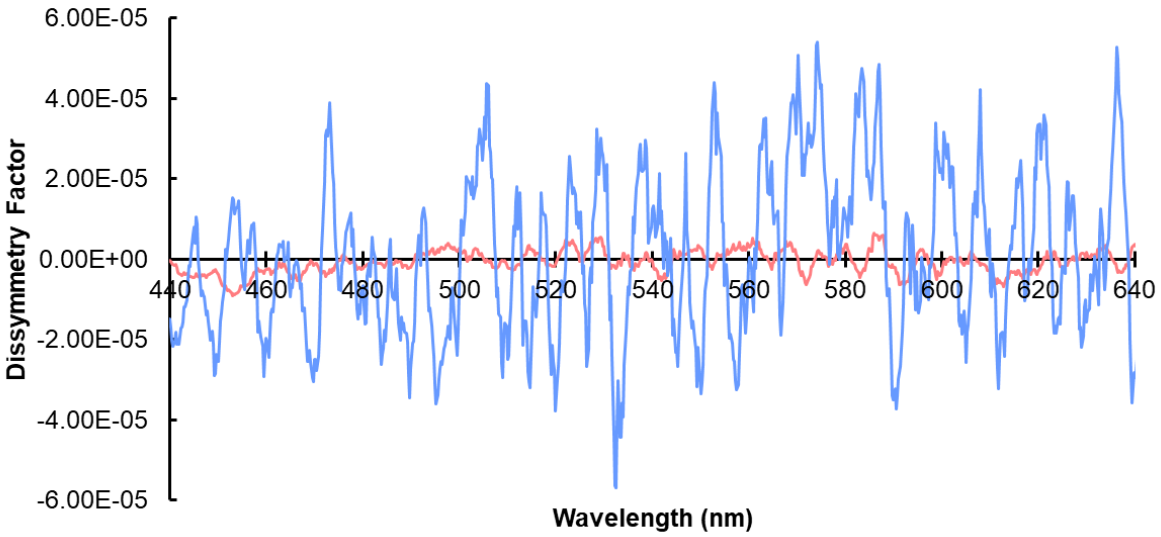

Figure S31. Normalized dissymmetry factor of ^{D}-iodide (bottom, pink) and ^{L}-iodide (top, blue) as a function of wavelength (5.0×10^{-3} mol L^{-1} in THF, λ_{ex} = 355 nm, band pass = 13 nm)

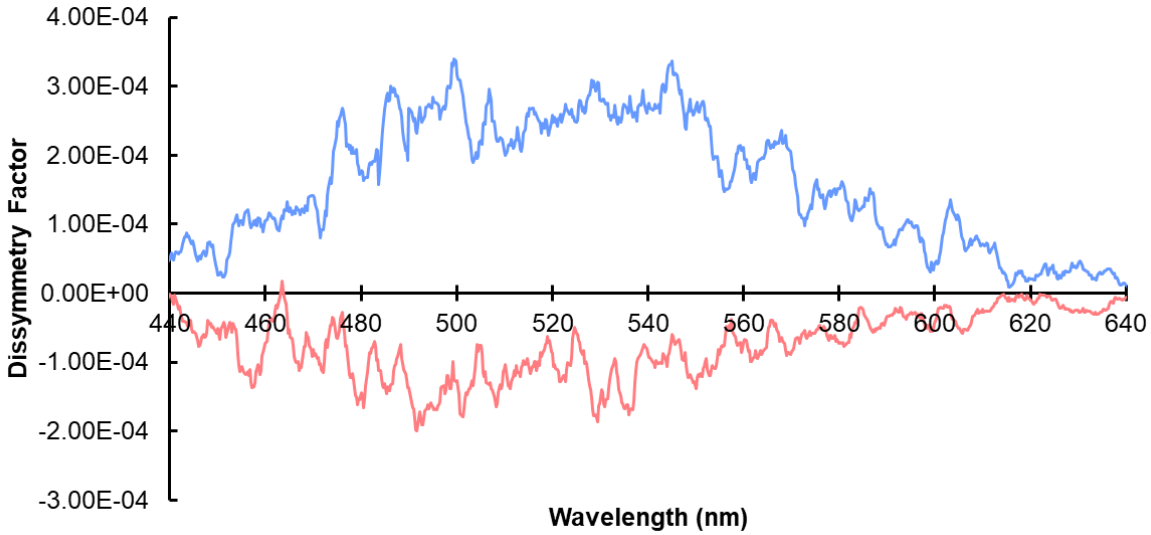

Figure S32. Normalized dissymmetry factor of ^{D}-B_3H_8 (bottom, pink) and ^{L}-B_3H_8 (top, blue) as a function of wavelength (5.0×10^{-3} mol L^{-1} in THF, λ_{ex} = 355 nm, band pass = 13 nm)

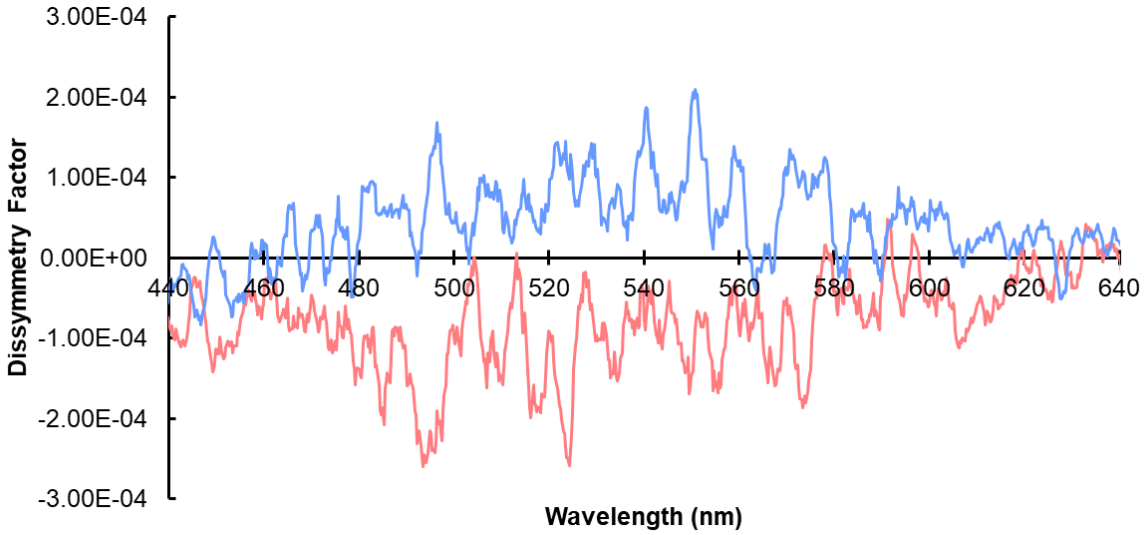

Figure S33. Normalized dissymmetry factor of ^{D}-BH_4 (bottom, pink) and ^{L}-BH_4 (top, blue) as a function of wavelength (5.0×10^{-3} mol L^{-1} in THF, λ_{ex} = 355 nm, band pass = 13 nm)

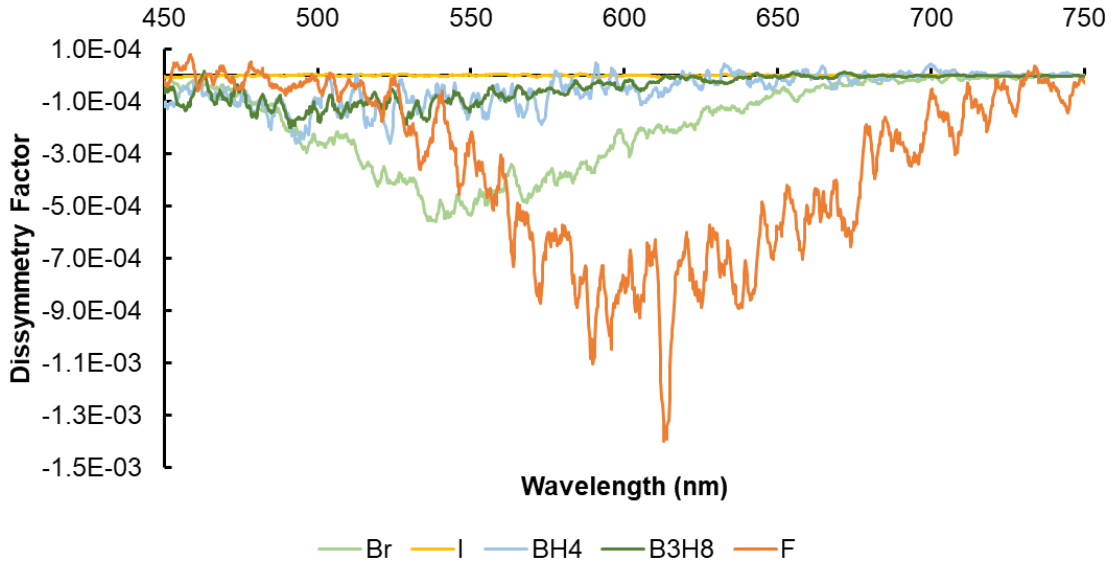

Figure S34. Normalized dissymmetry factor of all D isomers stacked for reference of g_{lum} values (5.0×10^{-3} mol L^{-1} in THF, λ_{ex} = 355 nm, band pass = 13 nm)

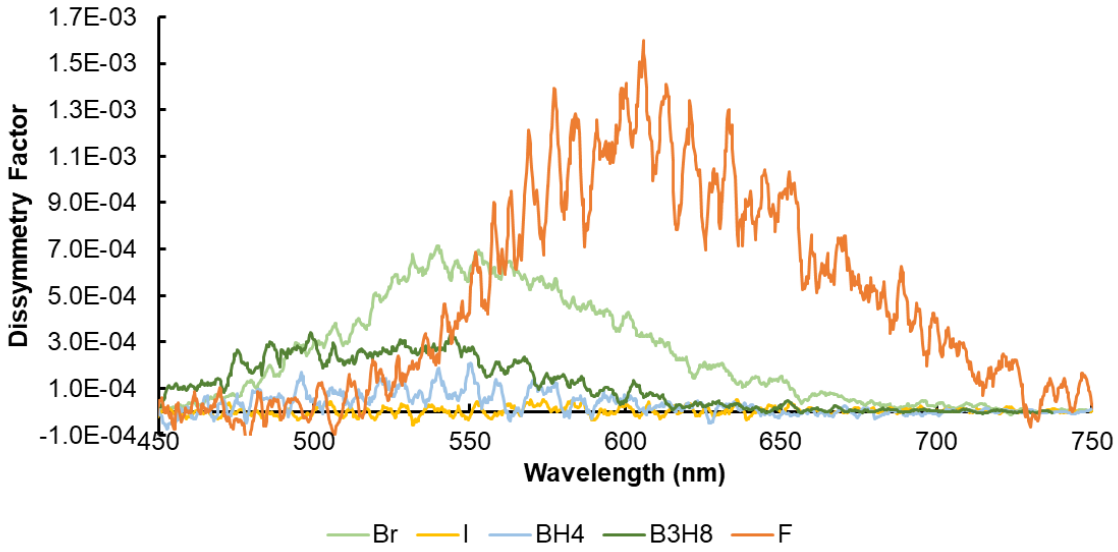

Figure S35. Normalized dissymmetry factor of all L isomers stacked for reference of g_{lum} values (5.0×10^{-3} mol L^{-1} in THF, λ_{ex} = 355 nm, band pass = 13 nm)

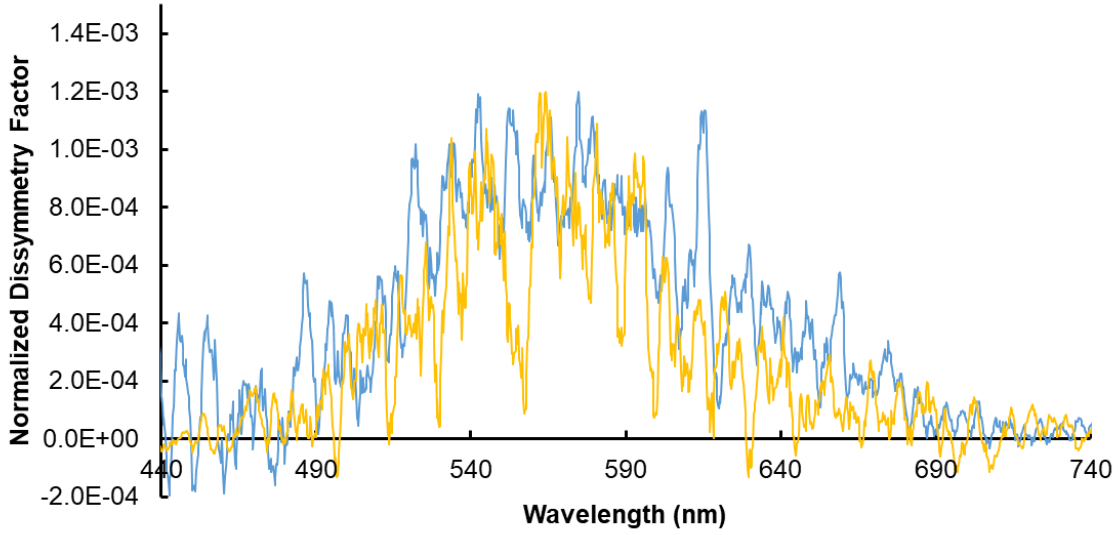

Figure S36. Normalized dissymmetry factor of ^{L}-chloride in benzene (yellow) and acetonitrile (blue) to demonstrate the effect of solvent on g_{lum} (5.0×10^{-3} mol L^{-1}, λ_{ex} = 355 nm, band pass = 13 nm)

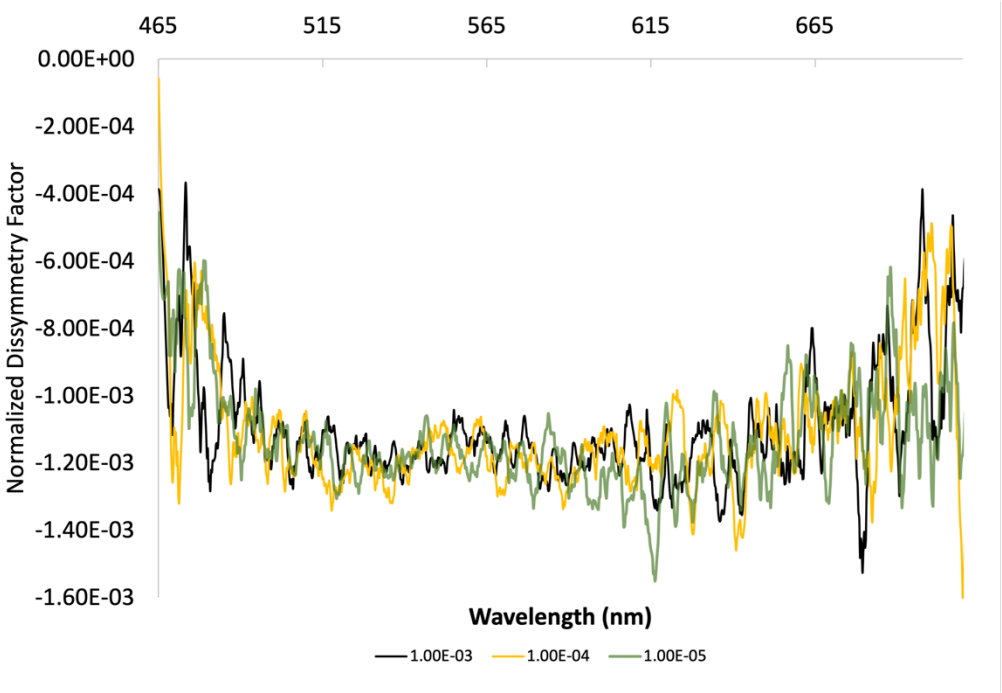

Figure S37. Normalized dissymmetry factor of ^{L}-chloride in THF to demonstrate the effect of concentration on g_{lum} (1.00×10^{-3}, 1.00×10^{-4}, 1.00×10^{-5}, mol L^{-1}, λ_{ex} = 355 nm, band pass = 13 nm)
Normalized dissymmetry factor (g_{lum}) was depicted for all CPL spectra for better graphical representation. This is obtained by plotting ΔI ($I_L - I_R$) but normalizing its maximum to the maximum g_{lum} calculated.

Circular Dichroism

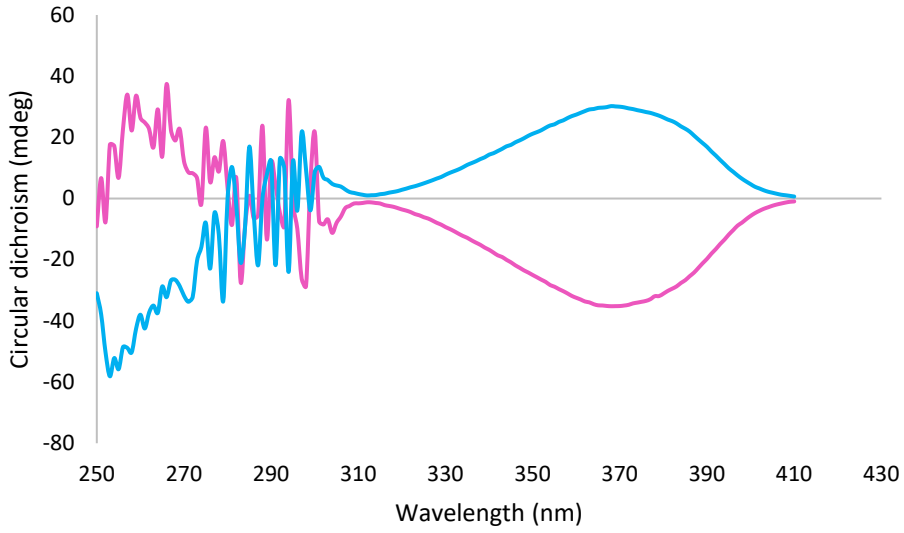

Figure S38. ECD spectrum of ^{L}-F (blue) and ^{D}-F (pink) in THF solutions (1.3 x 10^{-3} M) at RT

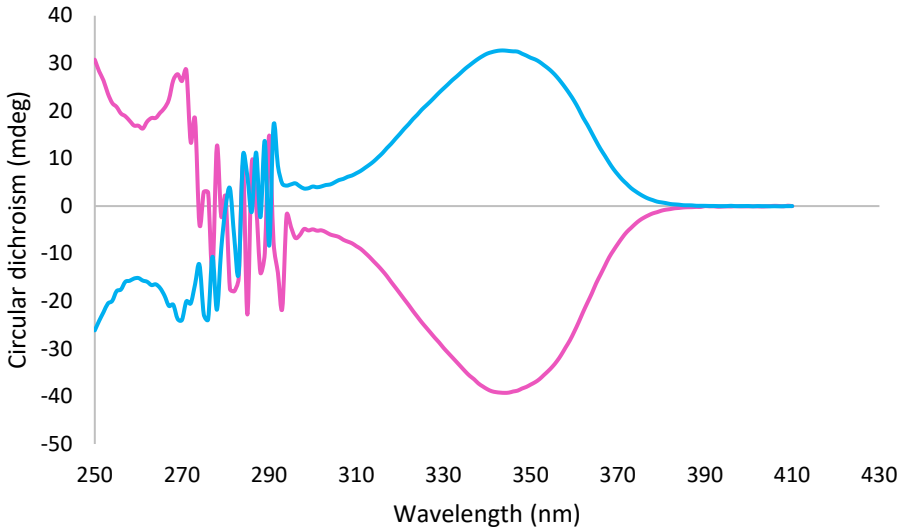

Figure S39. ECD spectrum of ^{L}-Br (blue) and ^{D}-Br (pink) in THF solutions (7.6 x 10^{-4} M) at RT

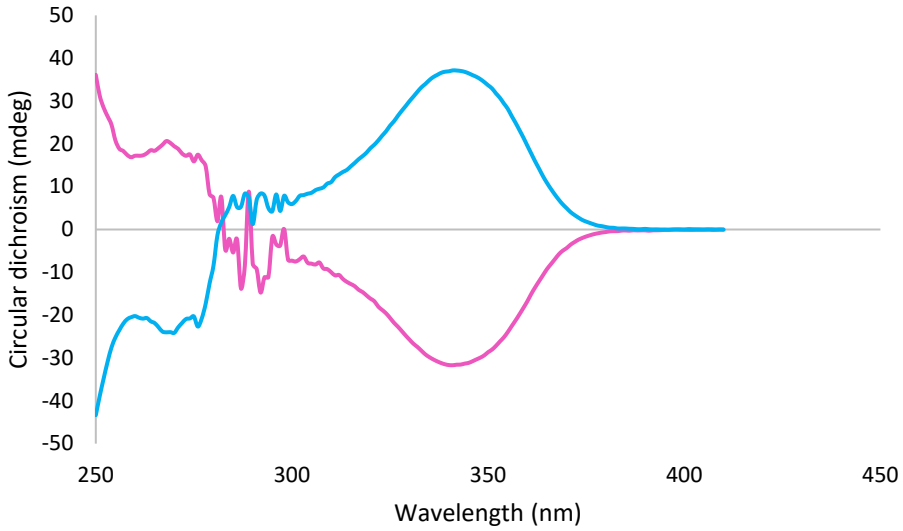

Figure S40. ECD spectrum of ^{L}-I (blue) and ^{D}-I (pink) in THF solutions (1.0 x 10^{-3} M) at RT

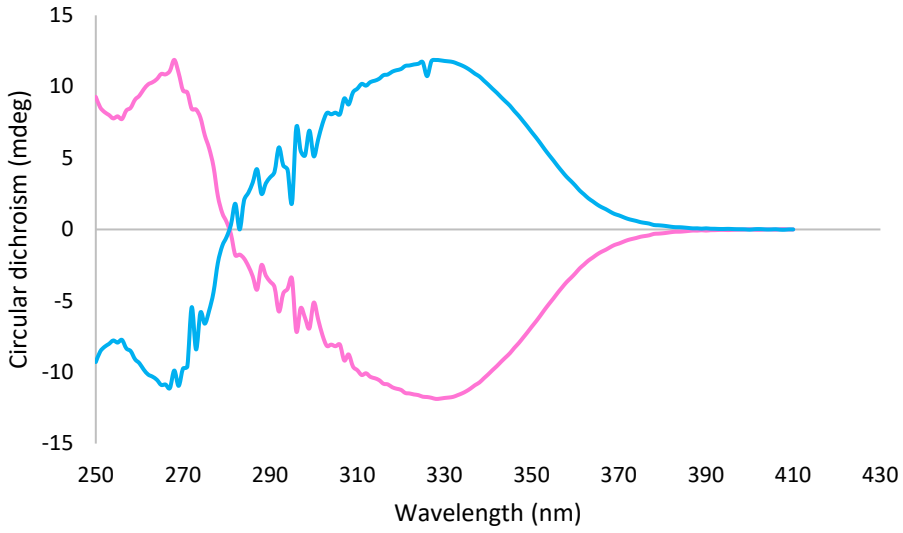

Figure S41. ECD spectrum of ^{L}-BH_4 (blue) and ^{D}- BH_4 (pink) in THF solutions (1.0 x 10^{-3} M) at RT

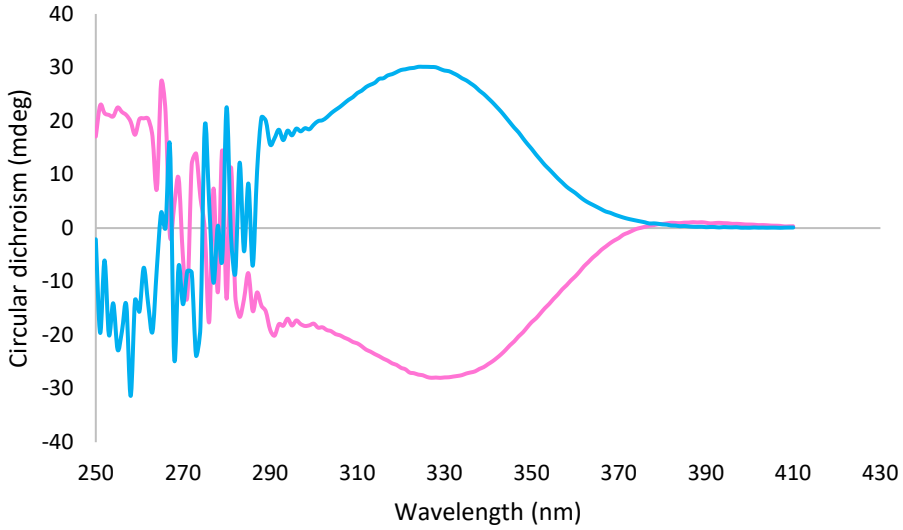

Figure S42. ECD spectrum of ^{L}-B_3H_8 (blue) and ^{D}- B_3H_8 (pink) in THF solutions (2.5 x 10^{-3} M) at RT

Absorbance Measurements

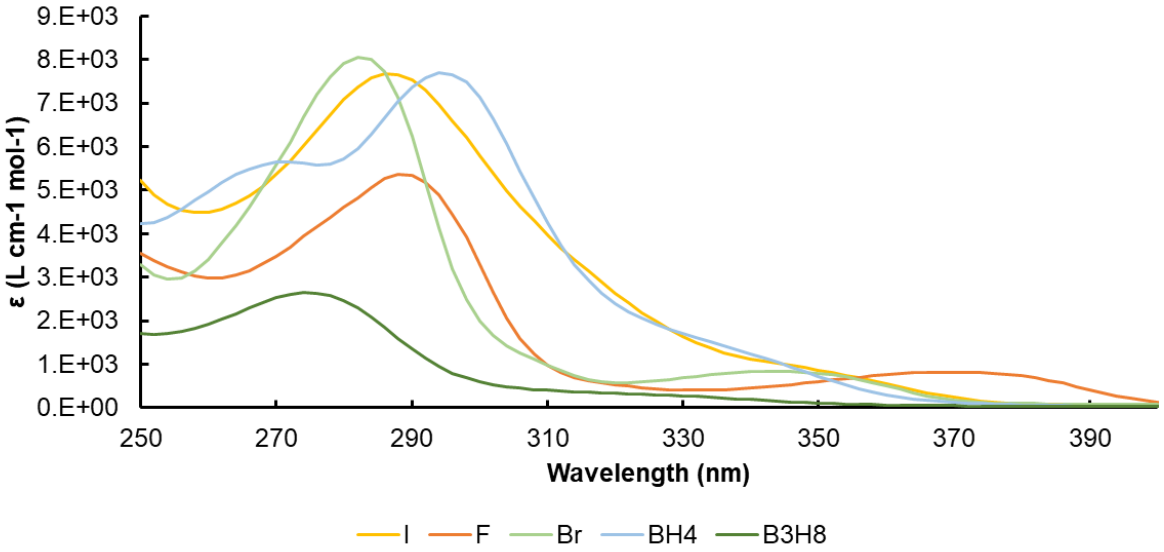

Figure S43. Absorbance of CAAC complexes in terms of molar absorptivity (ε) (1.2 × 10^{-4} mol L^{-1} in THF, λ_{ex} = 275 nm, slit width ex/em = 10/10 nm)

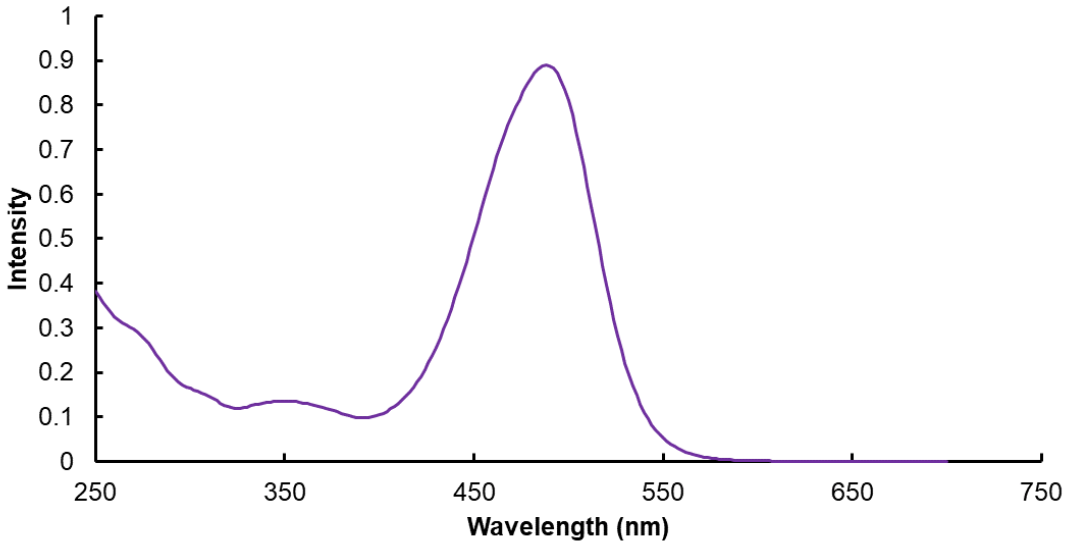

Figure S44. Absorbance of $[^{DMent}CAAC\text{-}Cu\text{-}H]_2$ (1.2 × 10^{-4} mol L^{-1} in THF, λ_{ex} = 275 nm, slit width ex/em = 10/10 nm)

Emission Measurements

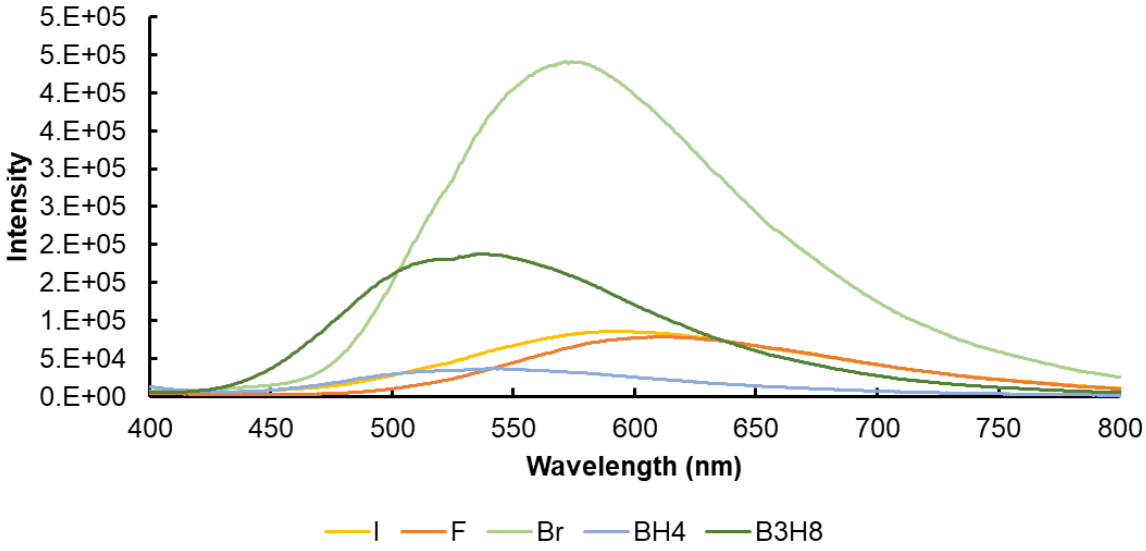

Figure S45. Emission of CAAC complexes (1.2×10^{-4} mol L^{-1} in THF, λ_{ex} = 270 nm, slit width ex/em = 10/10 nm)

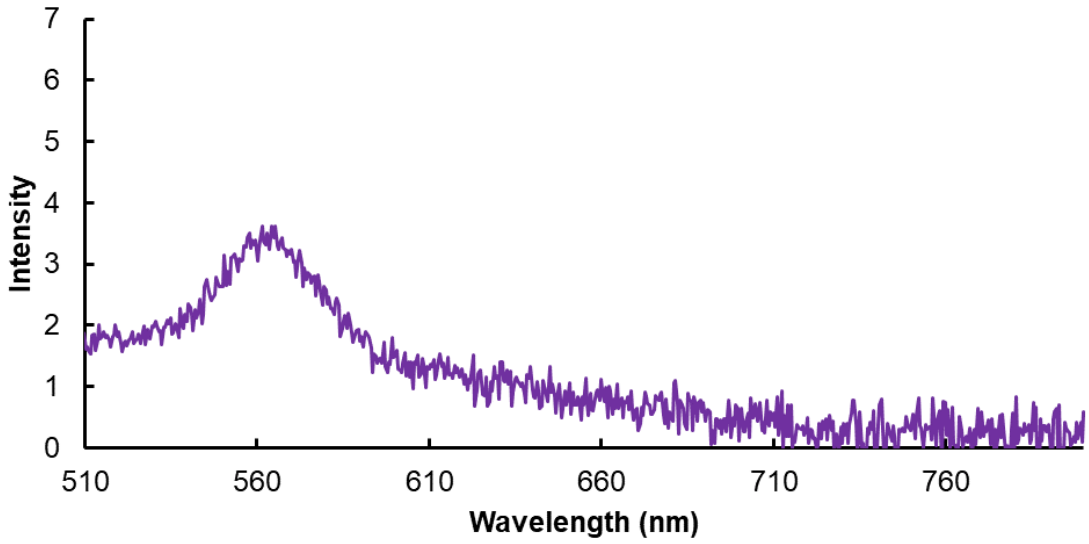

Figure S46. Emission of $[^{DMent}CAAC\text{-}Cu\text{-}H]_2$ (1.2×10^{-4} mol L^{-1} in THF, λ_{ex} = 490 nm, slit width ex/em = 10/10 nm)

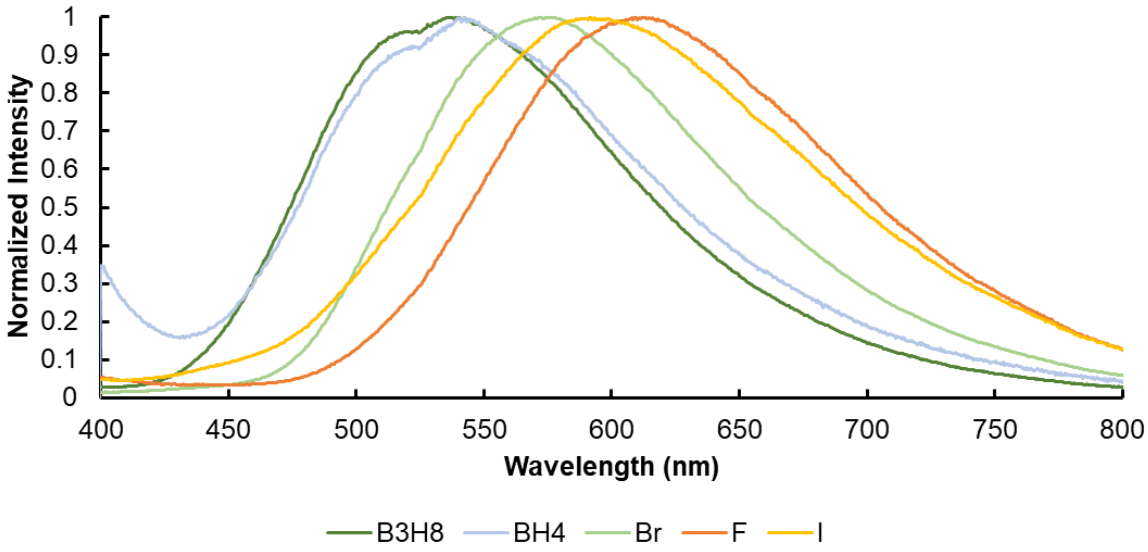

Figure S47. Normalized emission of CAAC complexes (1.2×10^{-4} mol L^{-1} in THF, λ_{ex} = 270 nm, slit width ex/em = 10/10 nm)

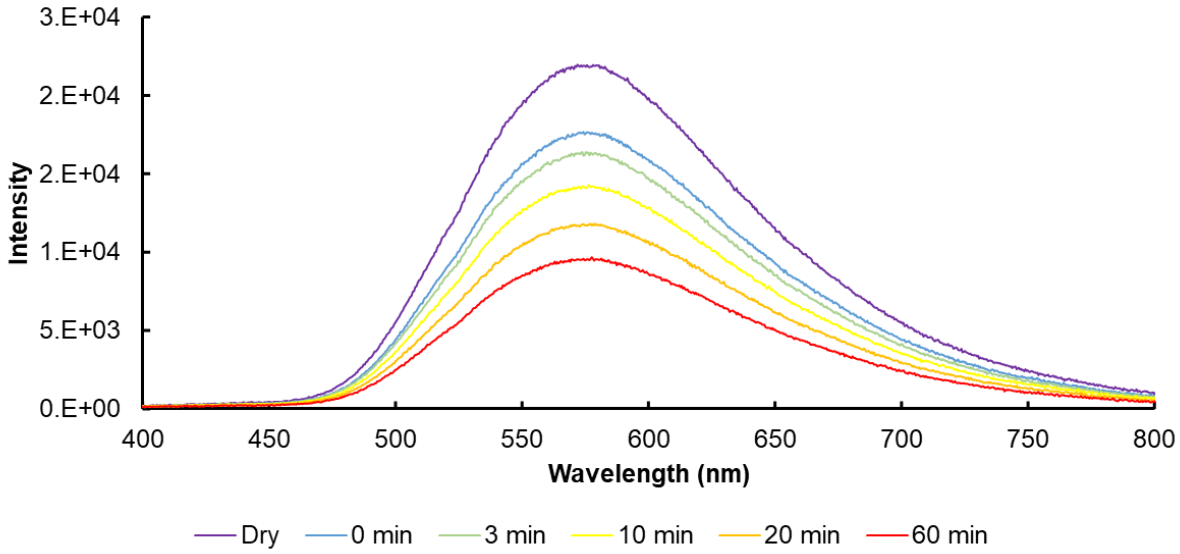

Figure S48. Emission of CAAC-Cu-Cl (5.0×10^{-3} mol L^{-1} in THF, λ_{ex} = 270 nm, slit width ex/em = 5/5 nm) in dry solvent, immediately after bubbling dehydrated air (1 mL) into the cuvette, 3 minutes after, 10 minutes after, 20 minutes after, and 60 minutes after.

Cyclic Voltammetry Measurements

All CV spectra were collected using a glassy carbon working electrode, a platinum counter electrode, and a silver reference electrode under inert atmosphere at room temperature and a scan rate of 0.1 V/s. All were calibrated to ferrocene in THF. Solutions were prepared as 1 mM sample in 0.1 M electrolyte ($TBAPF_6$) in THF. Solutions were stirred prior to any collection of data.

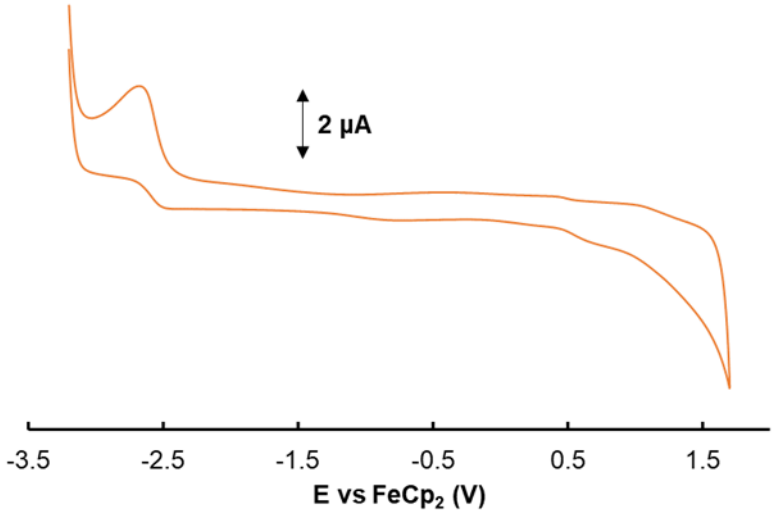

Figure S50. Cyclic voltammogram of ^{L}-F

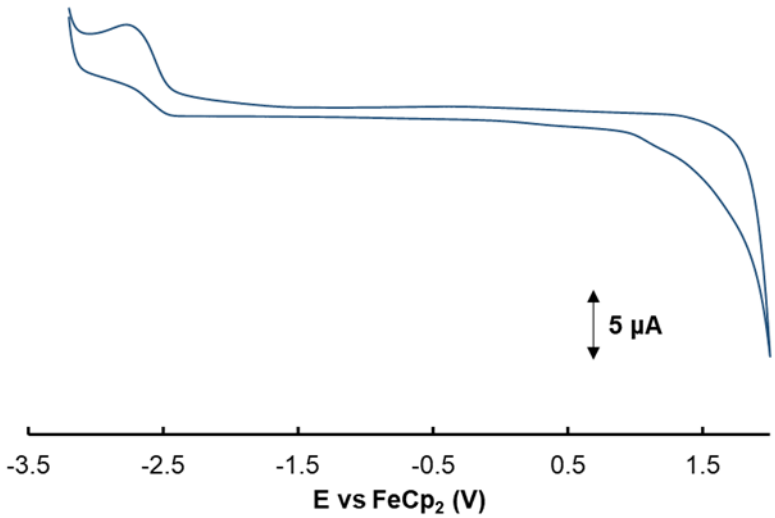

Figure S51. Cyclic voltammogram of ^{L}-Cl

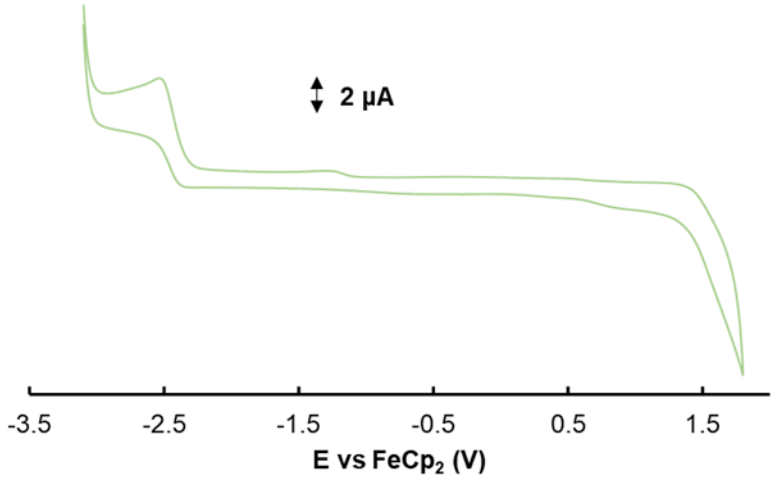

Figure S52. Cyclic voltammogram of ^{L}-Br

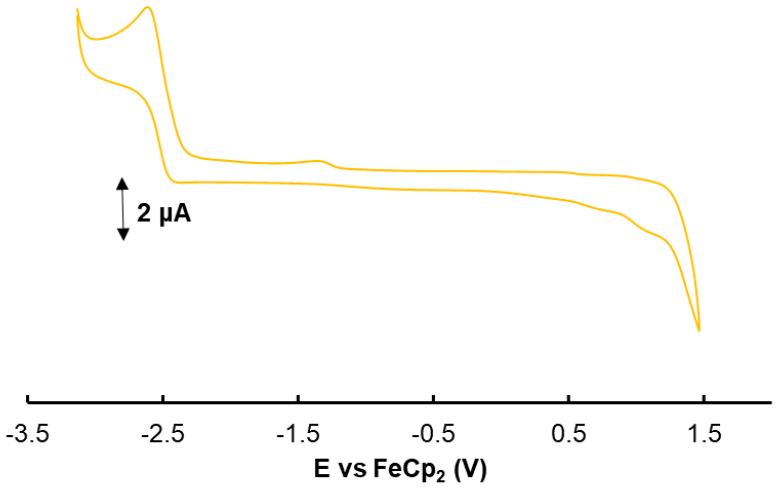

Figure S53. Cyclic voltammogram of ^{L}-I

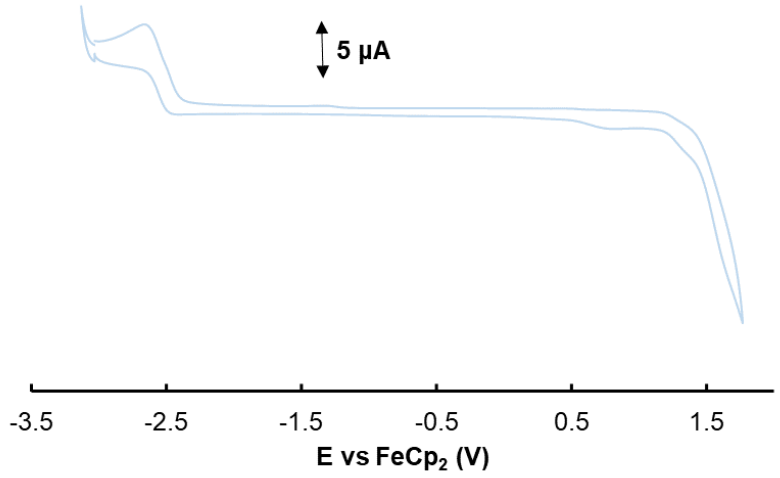

Figure S54. Cyclic voltammogram of ^{L}-BH_4

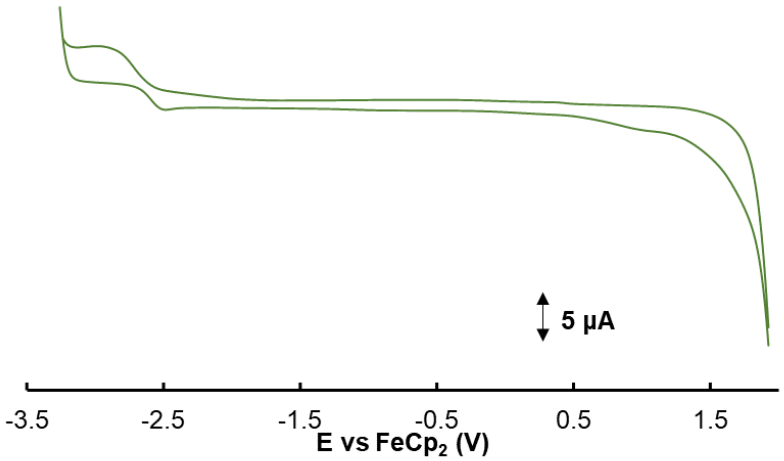

Figure S55. Cyclic voltammogram of ^{L}-B_3H_8

Table S1. Compiled onset potentials and band gap values obtained from CV data.

Complex	Reduction	E_{LUMO}	Oxidation	E_{HOMO}	ΔE
^{L}-F	-2.61	-2.78	0.66	-6.05	3.27
^{L}-Cl	-2.68	-2.71	0.52	-5.91	3.2
^{L}-Br	-2.48	-2.91	0.55	-5.94	3.03
^{L}-I	-2.57	-2.82	0.61	-6	3.18
^{L}-BH_4	-2.6	-2.79	0.64	-6.03	3.24
^{L}-B_3H_8	-2.64	-2.75	0.57	-5.96	3.21

Lifetime, Quantum Yield, and Brightness Data

Table S2. Lifetimes (τ, μs), quantum yields (φ, %), and brightness (B, L mol^{-1} cm^{-1}) for each CAACCu-X complex.

	I	Br	F	BH_4	B_3H_8
φ	0.8%	3.8%	2.1%	1.6%	6.2%
τ (μs)	1.39	5.20	4.09	0.599	5.68
B ($L \cdot mol^{-1} \cdot cm^{-1}$)	1.2×10^{-3}	7.4×10^{-2}	8.6×10^{-2}	1.4×10^{-2}	2.2×10^{-2}

Quantum yields were determined via a reference method, utilizing 1,9-diphenyl-anthracene as an external standard. Quantum yields were determined using the following equation:

$$\varphi_{Cu} = \varphi_{Std} \times (m_{Cu}/m_{Std}) \times (\eta_{Cu}/\eta_{Std})^2 \quad \text{(equation 2)}$$

Where subscripts Cu and Std denote the sample and standard respectively, φ is the quantum yield, m is the slope of the plot for the integrated emission vs absorbance, and η is the refractive index of the solvent. The calculated quantum yields can be found in Table S1.

$$B = \varphi \times \varepsilon \times (g_{lum}/2) \quad \text{(equation 3)}$$

Brightness (B) is determined by equation 3, where φ is the quantum yield, ε is the molar absorptivity, and g_{lum} is the dissymmetry factor.

X-ray Diffraction Data

Table S2. XRD data for ^{LMent}CAAC-Cu-Br

Identification code	^{LMent}CAAC-Cu-Br
Empirical formula	$C_{27}H_{43}BrCuN$
Formula weight	525.07
Temperature/K	100.00(10)
Crystal system	monoclinic
Space group	$P2_1$
a/Å	9.1460(3)
b/Å	15.0604(4)
c/Å	9.6356(2)
α/°	90

β/°	94.032(3)
γ/°	90
Volume/Å^3	1323.94(6)
Z	2
ρ_{calc}g/cm^3	1.317
μ/mm^{-1}	2.347
F(000)	552.0
Crystal size/mm^3	0.299 × 0.258 × 0.188
Radiation	MoKα (λ = 0.71073)
2Θ range for data collection/°	5.028 to 60.39
Index ranges	-12 ≤ h ≤ 11, -20 ≤ k ≤ 20, -13 ≤ l ≤ 13
Reflections collected	25910
Independent reflections	7040 [R_{int} = 0.0451, R_{sigma} = 0.0481]
Data/restraints/parameters	7040/1/280
Goodness-of-fit on F^2	1.063
Final R indexes [I>=2σ (I)]	R_1 = 0.0548, wR_2 = 0.1282
Final R indexes [all data]	R_1 = 0.0613, wR_2 = 0.1329
Largest diff. peak/hole / e Å^{-3}	0.58/-0.49
Flack parameter	-0.009(15)

Table S3. XRD data for ^{LMent}CAAC-Cu-I

Identification code	^{LMent}CAAC-Cu-I
Empirical formula	$C_{27}H_{43}CuIN$
Formula weight	572.06
Temperature/K	100.00(10)
Crystal system	monoclinic
Space group	$P2_1$
a/Å	9.2636(3)
b/Å	14.9564(3)
c/Å	9.8685(3)
α/°	90
β/°	98.276(3)

γ/°	90
Volume/Å^3	1353.05(7)
Z	2
ρ_{calc}g/cm^3	1.404
μ/mm^{-1}	1.961
F(000)	588.0
Crystal size/mm^3	0.276 × 0.19 × 0.131
Radiation	MoKα (λ = 0.71073)
2Θ range for data collection/°	4.444 to 60.706
Index ranges	-13 ≤ h ≤ 13, -20 ≤ k ≤ 20, -14 ≤ l ≤ 13
Reflections collected	26514
Independent reflections	7212 [R_{int} = 0.0459, R_{sigma} = 0.0471]
Data/restraints/parameters	7212/1/280
Goodness-of-fit on F^2	1.060
Final R indexes [I>=2σ (I)]	R_1 = 0.0344, wR_2 = 0.0673
Final R indexes [all data]	R_1 = 0.0391, wR_2 = 0.0700
Largest diff. peak/hole / e Å^{-3}	1.36/-0.68
Flack parameter	-0.018(10)

Table S4. XRD data for ^{LMent}CAAC-Cu-BH$_4$

Identification code	^{LMent}CAAC-Cu-BH$_4$
Empirical formula	$C_{31}H_{55}BCuNO$
Formula weight	532.11
Temperature/K	99.9(3)
Crystal system	tetragonal
Space group	$P4_32_12$
a/Å	12.87995(3)
b/Å	12.87995(3)
c/Å	37.23734(13)
α/°	90
β/°	90
γ/°	90

Volume/Å^3	6177.42(4)
Z	8
ρ_{calc}g/cm^3	1.144
μ/mm^{-1}	1.141
F(000)	2320.0
Crystal size/mm^3	0.364 × 0.183 × 0.153
Radiation	CuKα (λ = 1.54184)
2Θ range for data collection/°	7.262 to 146.896
Index ranges	-13 ≤ h ≤ 15, -15 ≤ k ≤ 15, -45 ≤ l ≤ 46
Reflections collected	94612
Independent reflections	6213 [R_{int} = 0.0332, R_{sigma} = 0.0115]
Data/restraints/parameters	6213/167/387
Goodness-of-fit on F^2	1.075
Final R indexes [I>=2σ (I)]	R_1 = 0.0303, wR_2 = 0.0832
Final R indexes [all data]	R_1 = 0.0304, wR_2 = 0.0833
Largest diff. peak/hole / e Å^{-3}	0.49/-0.46
Flack parameter	-0.024(4)

Table S5. XRD data for ^{LMent}CAAC-Cu-B_3H_8

Identification code	^{LMent}CAAC-Cu-B_3H_8
Empirical formula	$C_{27}H_{51}B_3CuN$
Formula weight	485.65
Temperature/K	99.98(10)
Crystal system	monoclinic
Space group	$P2_1$
a/Å	9.26984(9)
b/Å	37.7494(3)
c/Å	9.29479(9)
α/°	90
β/°	118.7857(13)
γ/°	90

Volume/Å^3	2850.60(5)
Z	4
ρ_{calc}g/cm^3	1.132
μ/mm^{-1}	1.155
F(000)	1056.0
Crystal size/mm^3	0.422 × 0.326 × 0.281
Radiation	CuKα (λ = 1.54184)
2Θ range for data collection/°	4.682 to 147.032
Index ranges	-11 ≤ h ≤ 11, -45 ≤ k ≤ 46, -11 ≤ l ≤ 11
Reflections collected	32062
Independent reflections	10835 [R_{int} = 0.0206, R_{sigma} = 0.0197]
Data/restraints/parameters	10835/1/659
Goodness-of-fit on F^2	1.046
Final R indexes [I>=2σ (I)]	R_1 = 0.0217, wR_2 = 0.0569
Final R indexes [all data]	R_1 = 0.0217, wR_2 = 0.0569
Largest diff. peak/hole / e Å^{-3}	0.35/-0.24
Flack parameter	-0.017(6)

References

(1) Dolomanov, O. V; Bourhis, L. J.; Gildea, R. J.; Howard, J. A. K.; Puschmann, H. *J. Appl. Crystallogr.* **2009**, *42* (2), 339–341.

(2) Sheldrick, G. M. *Acta Crystallogr. Sect. A* **2008**, *64* (1), 112–122.

(3) W. Hall, J.; Seeberger, F.; F. Mahon, M.; K. Whittlesey, M. *Organometallics* **2019**, *39* (1), 227–233.

(4) Deng, M.; Mukthar, N. F. M.; Schley, N. D.; Ung, G. *Angew. Chemie Int. Ed.* **2020**, *59* (3), 1228–1231.

(5) Frey, G. D.; Donnadieu, B.; Soleilhavoup, M.; Bertrand, G. *Chem. – An Asian J.* **2011**, *6* (2), 402–405.